environmental microbiology

Environmental Microbiology (2019) **21**(8), 2787–2808 doi:10.1111/1462-2920.14618

The interplay between zinc and iron homeostasis in *Aspergillus fumigatus* under zinc-replete conditions relies on the iron-mediated regulation of alternative transcription units of *zafA* and the basal amount of the ZafA zinc-responsiveness transcription factor

Rocío Vicentefranqueira,[1] Fernando Leal,[1,2] Laura Marín,[1] Clara Inés Sánchez[1] and José Antonio Calera[1,2*]

[1]*Instituto de Biología Funcional y Genómica (IBFG-CSIC), Universidad de Salamanca, Salamanca, Spain.*
[2]*Departamento de Microbiología y Genética, Universidad de Salamanca, Salamanca, Spain.*

Summary

Aspergillus fumigatus **is a saprophyte fungus that typically grows on organic decaying matter but can also parasitize immunosuppressed hosts. This is explained, in part, by its great ability to take up Zn^{2+} ions from living tissues, which is induced by the ZafA transcription factor. This study shows that the ZafA-mediated regulation of fungal growth is also influenced by iron availability and that *A. fumigatus* is well adapted to grow in zinc-limiting and zinc-replete media with Zn:Fe ratios lower in the former than in the latter. Accordingly, this indicates that iron availability appears to be more critical for fungal growth in zinc-replete than in zinc-limiting environments. Interestingly, the cross-regulation of zinc/iron homeostasis under zinc-replete conditions relies on an unprecedented iron-mediated regulation of different *zafA* transcription units that, along with a limited transcript translation, allows synthesizing the right basal amount of ZafA dependent on iron availability. We posit that this regulatory strategy has evolved in fungi as a mechanism to adjust zinc intake to iron availability under zinc-replete conditions. Thus, fungal growth is enhanced in zinc- and iron-replete media but restricted by reducing zinc intake under iron starvation to prevent the noxious side effects of an intracellular zinc excess during iron deficiency.**

Received 1 October, 2018; accepted 3 April, 2019. *For correspondence. E-mail jacalera@usal.es; Tel. 34-923-294891; Fax 34-923-224876.

Introduction

Zinc is the second most widespread metal present in enzymes after magnesium (Andreini *et al.,* 2008). It is an essential nutrient for the normal functioning of hundreds of enzymes as a cofactor for their catalytic activity and/or structural stability (Andreini *et al.,* 2008; Auld, 2009). In addition, zinc is necessary for the functioning of regulatory proteins of superclass 2, which is by far the largest superclass of transcription factors that use Zn^{2+} ions for the correct folding and stability of their DNA-binding domains (Wingender, 2013). For these reasons, zinc is essential for a wide variety of biochemical reactions, cellular growth and development. When the cellular zinc content is lower than the 'zinc quota', that is, the total amount of zinc required for a cell to grow optimally (Outten and O'Halloran, 2001), cell growth stops. In contrast, when the cellular zinc content exceeds a maximum concentration, cells become intoxicated, most likely due to the nonspecific reactions of Zn^{2+} ions with the —SH groups of proteins.

Like all organisms, fungi tightly regulate zinc homeostasis to ensure an appropriate steady supply of zinc. *Aspergillus fumigatus* is a filamentous fungus that is able to grow in the lungs of immunosuppressed individuals and causes invasive pulmonary aspergillosis (Karthaus and Buchheidt, 2013). The ability to obtain zinc from host tissues is one of the most important biological traits that enables *A. fumigatus* to grow and cause disease in susceptible individuals (Amich *et al.,* 2014; Amich and Calera, 2014). The regulation of the homeostatic and adaptive response to zinc starvation in *A. fumigatus* is mediated by the ZafA transcription factor (Vicentefranqueira *et al.,* 2018), which is essential for fungal virulence (Moreno *et al.*, 2007b). ZafA regulates gene expression through binding to the zinc responsive (ZR) motifs present in the regulatory regions of its target genes (Vicentefranqueira *et al.,* 2018), as does the Zap1 transcription factor of *Saccharomyces cerevisiae*, which

is the best characterized ZafA orthologue to date (Zhao and Eide, 1997). The Zap1 regulon and the genes targeted directly by Zap1 have been well identified, and the mechanism of action of Zap1 has been studied in depth (Eide, 2009). However, it has not been reported that *ZAP1* expression is influenced by an environmental stimulus other than zinc starvation. In contrast, it is known that in zinc-replete media *zafA* expression is influenced by iron (Schrettl *et al.,* 2008; Schrettl *et al.,* 2010; Chung *et al.,* 2014). Intriguingly, in the absence of the *hapX*, *srbA* or *srbB* genes, which, respectively, encode the bZIP-type regulator HapX and the SrbA and SrbB sterol-regulatory element binding proteins (SREBP), *zafA* expression in zinc-replete, iron-limiting media is altered following an iron-shock (i.e., a sudden supplement of an iron-limiting media with a relatively high amount of iron) (Schrettl *et al.,* 2010; Blatzer *et al.,* 2011; Chung *et al.,* 2014). HapX regulates iron homeostasis, whereas SrbA and SrbB coordinately regulate iron homeostasis and ergosterol biosynthesis in response to hypoxia (Schrettl *et al.,* 2010; Blatzer *et al.,* 2011; Chung *et al.,* 2014). On the other hand, zinc starvation negatively influences the expression of genes encoding proteins involved in iron homeostasis and ergosterol biosynthesis including *hapX*, *srbA* and *srbB* (Vicentefranqueira *et al.,* 2018). Therefore, zinc/iron and zinc/ergosterol cross-regulatory networks appear to exist that would enable *A. fumigatus* to integrate and/or coordinate the adaptive response to changes in iron and ergosterol metabolism depending on zinc availability, even under zinc-replete conditions. However, it is unknown whether ZafA plays a role in regulating zinc homeostasis in zinc-replete media. In this work, we describe that the ZafA-mediated adaptation of *A. fumigatus* to grow in zinc-replete media is influenced by the environmental concentration of iron and propose a model to explain the underlying regulatory mechanism.

Results

Regulation of zinc homeostasis is influenced by iron availability

To investigate the effect of Zn and Fe availability on fungal physiology, we measured the growth ability of *A. fumigatus* in iron-limiting and iron-replete media under zinc-limiting and zinc-replete conditions (Fig. 1A). The growth capacity of a Δ*zafA* strain was significantly higher

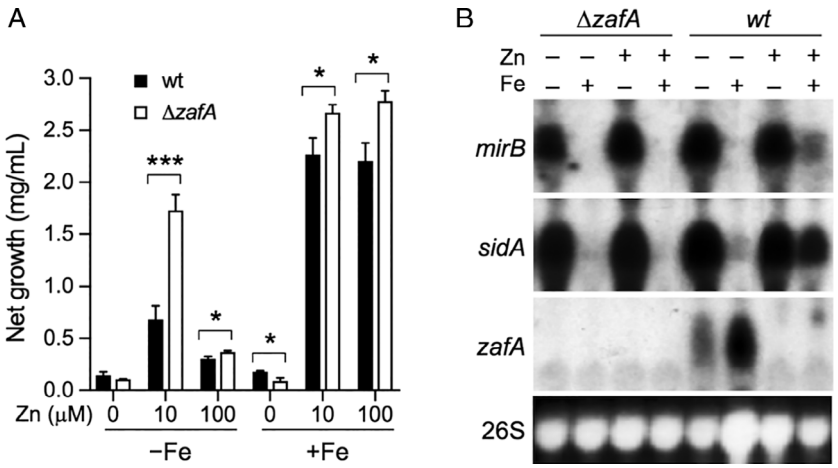

Fig. 1. Effect of zinc and iron on the growth ability of a Δ*zafA* mutant and the expression of genes related to iron uptake and regulation of zinc homeostasis.

A. Measurement of the growth capacity of a wild-type (AF14) and a Δ*zafA* strain (AF171) grown in liquid SDN–Zn–Fe supplemented with zinc and/or 50 μM iron, as indicated. Liquid cultures (20 ml) were set up in triplicate. Mycelia were harvested by filtration using GF/C filters, and the net dried weights were measured and plotted. Under iron-replete, zinc-limiting conditions, the wild-type strain reached a net growth that was significantly higher than that of a Δ*zafA* strain (*P = 0.0401). In contrast, in an iron-limiting medium supplemented with 10 μM Zn, a Δ*zafA* strain grew much better than the wild type strain (***P = 0.0003). The growth ability of both strains was also dramatically enhanced in an iron-replete medium supplemented with 10 μM and 100 μM zinc, even though in both cases the Δ*zafA* mutant reached net growths significantly higher than that of the wild type (*P = 0.0391 for 10 μM zinc; *P = 0.0111 for 100 μM Zn). The growth ability of both strains reduced dramatically in an iron-limiting medium supplemented with 100 μM Zn, although even under this condition the Δ*zafA* mutant reached a slightly, but statistically significant, higher net growth than that of the wild type (*P = 0.0367). Data were analysed statistically with the Prism 7.0 Software using a two-tailed, unpaired t test.

B. Total RNA was obtained from the strains cultured in the SDN–Zn–Fe medium with or without a supplement of 10 μM zinc and/or 50 μM iron. RNA was analysed by Northern blot. The DNA fragments used as probes for *sidA* and *mirB* were obtained by PCR using the pairs of oligonucleotides SIDA-D/SIDA-R1 (340 bp) and MIRB-D1/MIRB-R1 (462 bp), respectively, as primers and gDNA from strain AF14 as the template. A DNA fragment of 1038 bp, which was used as a probe for zafA, was obtained by PCR using the oligonucleotide pair JA57/JA58 and a diluted aliquot of the plasmid pZAF14 as template (Moreno et al., 2007b). The 26S rRNA was included as a loading control.

than that of a wild-type strain under zinc-replete conditions, regardless of iron availability. In contrast, the growth capacity of a Δ*zafA* strain was significantly lower than that of a wild-type strain in iron-replete media under zinc-limiting conditions. Consistent with this observation, the expression of prototypic genes related to iron uptake, such as *sidA* and *mirB*, was strongly induced in both strains under iron-limiting conditions, regardless of zinc availability (Fig. 1B). Conversely, the expression of these genes was completely repressed in the Δ*zafA* mutant but only partially repressed in the wild-type strain, particularly under zinc-replete conditions. These results indicated that the iron supplement added to a zinc-replete medium was enough to fulfil the iron requirement of a Δ*zafA* mutant but not enough to cover the iron demand of a wild-type strain. This suggested the existence of a ZafA-mediated regulatory mechanism that could be influenced by iron availability.

The Zn:Fe ratio of the medium determines fungal growth ability

To ascertain the influence of the Zn:Fe ratio of a medium on fungal growth, a wild-type strain was cultured in SDN–Zn–Fe medium containing 1, 10 and 100 μM Zn and increasing amounts of iron (Fig. 2A). It was found that the increasing amounts of the iron supplement only significantly enhanced fungal growth in media containing zinc concentrations ≥10 μM. To detect the effect of minute amounts of iron on fungal growth, the growth yield coefficients (Y) were calculated for iron with respect to the Zn:Fe ratio of the medium (Fig. 2B). The highest Y coefficient for iron in media containing 100, 10 and 1 μM Zn were, respectively, 388, 1214 and 1329 mg/μmol Fe, which were reached using Zn:Fe ratios of 63.6, 7.75 and 2.67. This suggested that an excess of zinc was noxious for the fungal growth under iron-limiting conditions. Moreover, the ability of the fungus to use iron to grow was reduced exponentially depending on the Zn:Fe ratio of the medium (Fig. 2C). In addition, these results showed that although *A. fumigatus* grows optimally in media containing 10 μM Zn and 1.29 μM Fe (i.e., at a Zn:Fe ratio of 7.75), it can also grow well in media with a broad range of zinc and iron concentrations, which is consistent with the interconnected regulation of zinc and iron homeostasis.

Regulation of zinc and iron homeostasis is strongly influenced by the Zn:Fe ratio of the medium

To investigate the relationship between the Zn:Fe ratio of a medium and the regulation of zinc and iron homeostasis at the transcriptional level, we analysed the expression of *sidA* and *zafA* in the fungus grown in the presence of three different concentrations of zinc and increasing amounts of iron (Fig. 3A) and in the presence of three different concentrations of iron and increasing amounts of zinc (Fig. 3B). The transcription level of *sidA* decreased as the iron supplement increased, regardless of the amount of zinc present in the media. However, the expression of *sidA* was detected in media supplemented with ≥10 μM zinc even in the presence of relatively high amounts of iron. The transcription of *sidA* was detected in all media with a Zn:Fe ratio content ≥0.1 and only became fully repressed by 100 μM iron in media containing ≤1 μM Zn. In contrast, the transcription level of *zafA* increased in media containing ≤1 μM Zn until the concentration of the iron supplement reached ~6.0 μM, whereas *zafA* expression became fully repressed in media containing ≥10 μM zinc (regardless of the amount of iron in the media). Interestingly, these experiments revealed the unprecedented discovery that *zafA* was transcribed in two different types of transcripts depending on zinc availability. A set of transcripts of ~1.9-2.1 kb (designated collectively as S, for Short transcripts or S-mRNAs) were synthesized in media containing ≤3 μM Zn, whereas another set of transcripts of ~2.2-2.6 kb (designated collectively as L, for Long transcripts or L-mRNAs) were synthesized in media containing ≥10 μM zinc.

ZafA has two transcription units

To show that the different types of *zafA* transcripts were the products of two alternative overlapping transcription units of *zafA*, RNA samples obtained from a wild-type strain grown in a zinc- and iron-limiting media supplemented with increasing amounts of zinc and iron were analysed in duplicate by Northern blot using two different probes (L and LS) (Fig. 4A). As expected, the L-probe only detected the L-transcripts under zinc-replete conditions, whereas the LS-probe detected both the L-transcripts (under zinc-replete conditions) and the S-transcripts (under zinc-limiting conditions). Therefore, *zafA* had two transcription units (S and L) that were expressed differentially depending on zinc availability: (i) The S-transcripts expressed exclusively under zinc-limiting conditions and (ii) the L-transcripts expressed under zinc-replete conditions. In addition, it was noticeable that the expression of the Shortest L-transcripts (SL-mRNAs; ~2.2-2.3 kb) was detected under both iron-limiting and iron-replete conditions, while the expression of the Longest L-transcripts (LL-mRNAs; ~2.3-2.6 kb) was only detected under iron-limiting conditions.

Both types of transcripts showed extended smears upon separation in agarose-formaldehyde gels. However, they both had similar 3′-polyadenylation sites (PS) as shown by 3′-RACE (Supporting Information Fig. S1A), which indicated they had to have multiple 5′ transcription

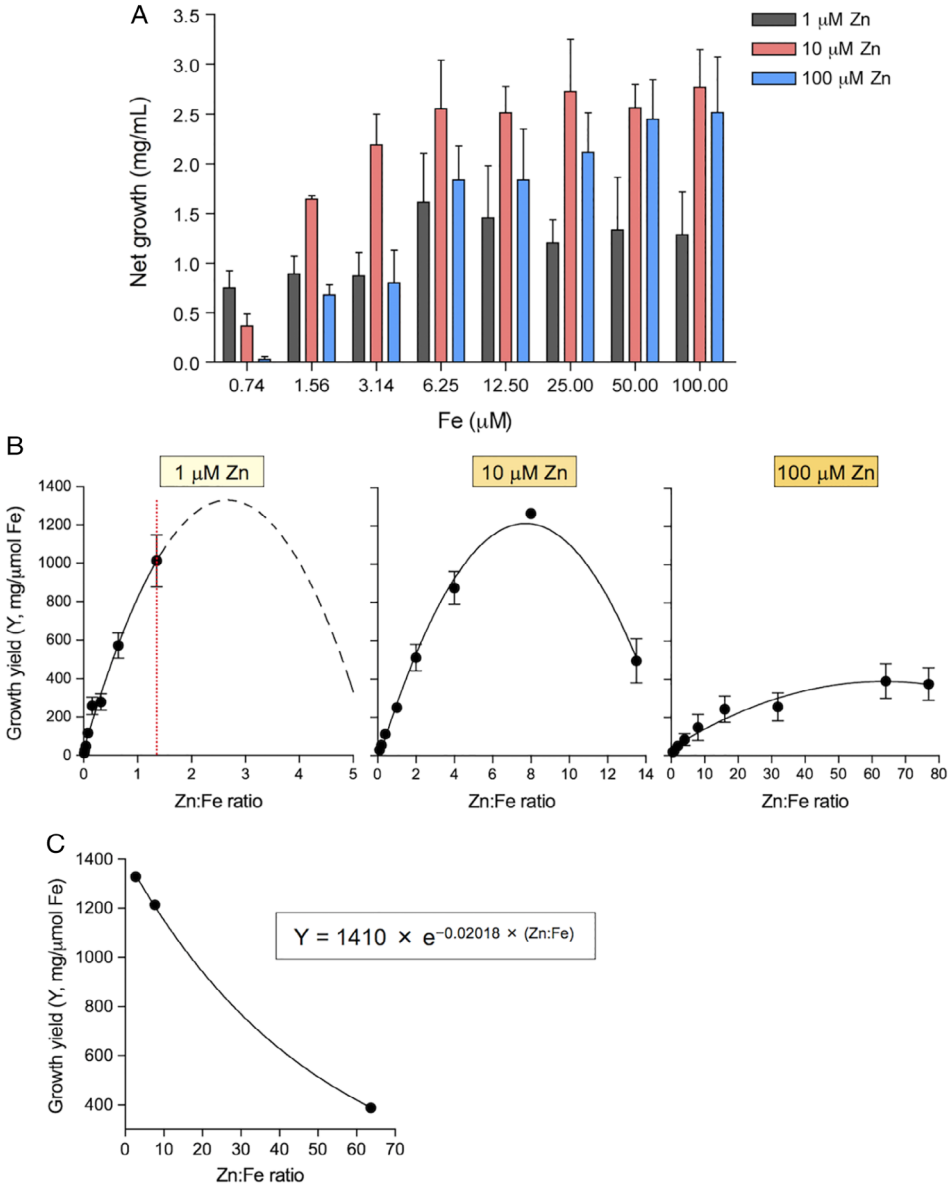

Fig. 2. Influence of the Zn:Fe ratio of the culture medium on fungal growth.
A. Measurement of the growth ability of a wild-type strain (AF14) in liquid SDN–Zn–Fe containing the indicated amounts of zinc and iron. It must be noted that the SDN–Zn–Fe medium contains 0.74 μM iron. Liquid cultures (20 ml) were set up in triplicate. Mycelia were harvested by filtration and the net dried weights were measured and plotted. Data were analysed statistically with the Prism 7.0 Software using a one-way ANOVA test. Overall, in the media containing 1 μM Zn, the increase of the iron supplement did not enhance significantly the net fungal growth (P = 0.143). In contrast, in media containing both 10 and 100 μM Zn any increase of the iron supplement enhanced significantly the net fungal growth (P = 0.0012) until they reached a plateau in media supplemented with either 10 μM Zn plus ≥3.14 μM Fe or 100 μM Zn plus ≥6.25 μM Fe.
B. Representations of the growth yield coefficients for iron with respect to the Zn:Fe ratio in SDN–Zn–Fe supplemented with 1, 10 and 100 μM Zn and increasing amounts of iron. The Y coefficient showed the amount of biomass produced (as mg of mycelium) per substrate unit (as μmoles of iron). The relationship between the Y values and Zn:Fe ratios fitted to second-order polynomial regression equations (R^2 = 0.972 for 10 μM; R^2 = 0.801 for 100 μM), as determined using the Prims 7.0 software. We could not directly determine the Y coefficients for iron supplements lower than 0.74 μM in media containing 1 μM Zn, that is, with a Zn:Fe ratio higher than 1.35 (indicated by a red line). Instead, we applied the second-order polynomial regression equation that specifically correlated the Y coefficient with the Zn:Fe ratio of a medium containing 1 μM Zn when using iron supplements <0.74 μM (R^2 = 0.928), to extrapolate the corresponding curve (broken line in the left panel).
C. The growth yield for iron was inversely proportional to the Zn:Fe ratio of the medium. The data fitted very well to an exponential growth equation (R^2 = 0.999), as determined using the Prims 7.0 software. [Color figure can be viewed at wileyonlinelibrary.com]

start sites (TSSs). All the TSSs for the S-transcripts were mapped between positions −278 and −42 in the gDNA, with the major TSS located at position −44 (Fig. 4B and Supporting Information Fig. S1B). The TSSs for the L-transcripts mapped between positions −833 and −441 in the gDNA, with the major TSS being positioned at −618

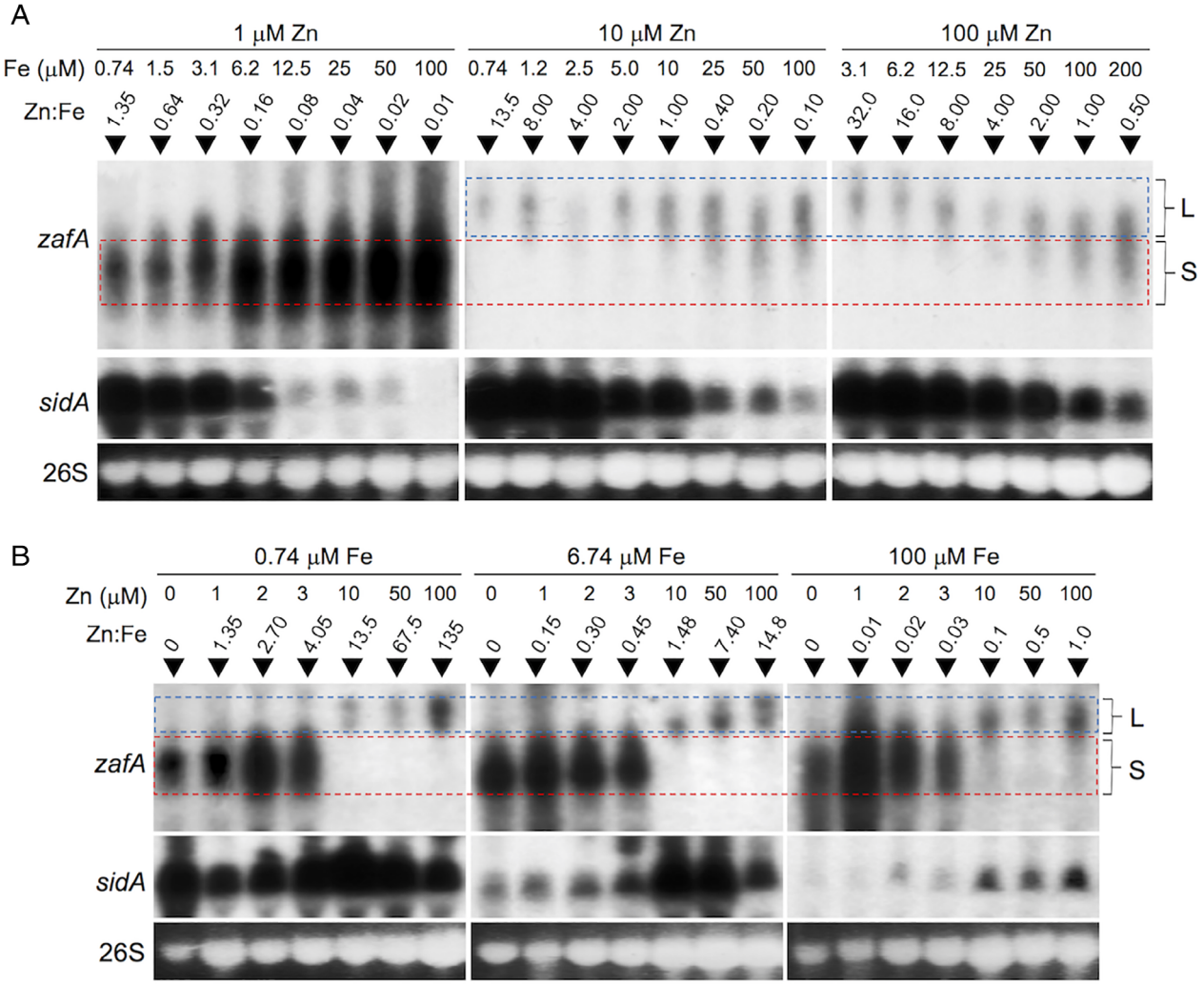

Fig. 3. Influence of the Zn:Fe ratio of the medium on the expression of *zafA* and *sidA.*
A. Total RNA was obtained from the AF14 strain cultured in the SDN–Zn–Fe medium containing 1, 10 and 100 μM Zn and increasing amounts of iron, as indicated.
B. Total RNA was obtained from the AF14 strain cultured in the SDN–Zn–Fe medium containing 0.74, 6.74 and 100 μM iron and increasing amounts of zinc as indicated. The RNA samples were analysed by Northern blot. The DNA fragments used as probes for *sidA* and *zafA* were obtained by PCR as previously described. The signals corresponding to the L- and S-transcripts in the blots were delimitated approximately by a blue and red box, respectively. The 26S rRNA was included as a loading control. [Color figure can be viewed at wileyonlinelibrary.com]

(Fig. 4B and Supporting Information Fig. S1B). Although there was not a clear boundary between LL and SL-mRNAs, two regions were observed in the *zafA* promoter sequence where the TSSs of the L-transcripts appeared to be concentrated. This in turn allowed the TSSs for the LL- and SL-transcripts to be defined; the former was located within and upstream of the ZRR3 motif (Fig. 4B) and the latter was located downstream of this ZafA binding motif (Vicentefranqueira *et al.,* 2018). In addition, there were two 5′-UTR Intronic Sequences with a length of 53 bp (UIS1) and 106 bp (UIS2) (Fig. 4B and Supporting Information Fig. S1B). Interestingly, in the S-transcripts, the first AUG corresponded to the in-frame translation start codon (Fig. 4C), whereas the L-mRNAs had from one to five out-of-frame AUG codons with a weighted average of 2.8 out-of-frame AUG codons per transcript (Supporting Information Fig. S1B). More precisely, the SL- and LL-mRNAs had between 1-3 and 3-5 out-of-frame AUG codons (Fig. 4C), respectively.

ZafA induces the transcription of the S-transcripts while that of the L-transcripts occurs in a ZafA-independent manner

To investigate whether ZafA regulated the expression of the S- and L-mRNA transcripts, we constructed strains AF1031 and AF1043 (Supporting Information Figs. S2

and S3). The *zafA* coding sequence in these strains had been replaced by that of the sGFP (Fernández-Ábalos *et al.,* 1998). In addition, the AF1043 strain carried a *myc*-tagged wild-type version of the *zafA* coding sequence at its *pyrG* locus under the control of the *zafA* promoter (Supporting Information Fig. S3 and Fig. 5A).

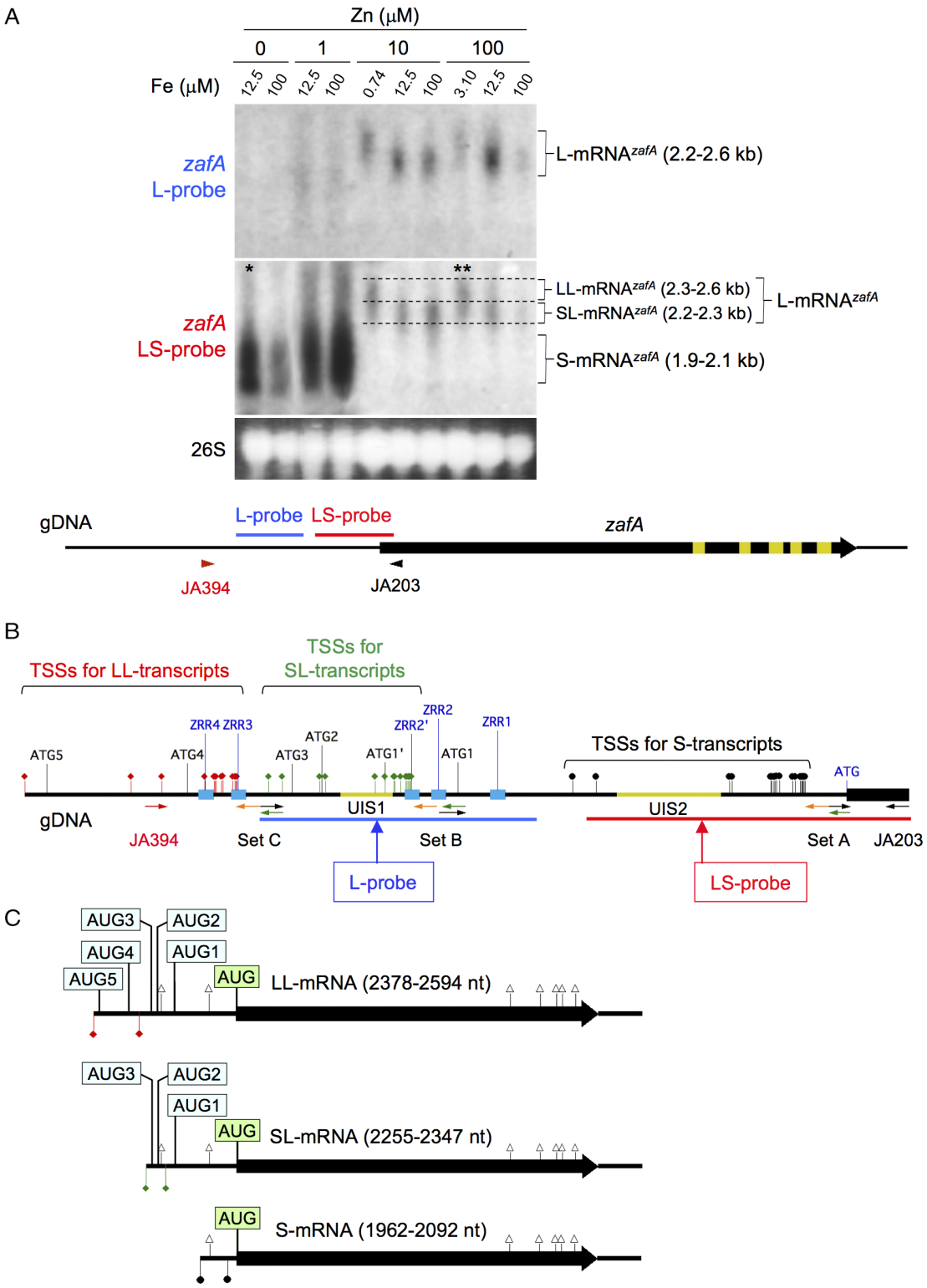

We analysed the effect of a zinc-shock (i.e., a sudden supplement of a zinc-limiting media with a high amount of zinc) on the S-mRNA → L-mRNA transcriptional shift (Fig. 5B). The expression of these *zafA* transcripts in AF1043 was analysed using an appropriate *zafA* probe to detect both the S- and the L-mRNA$^{myc\text{-}zafA}$ transcripts (Fig. 5B; Blot #1). The expression of the S-mRNA$^{myc\text{-}zafA}$ transcripts dropped to undetectable levels 20 min after the zinc shock, whereas the L-mRNA$^{myc\text{-}zafA}$ transcripts became detectable 6 h after the zinc shock. Another identical blot membrane was hybridized in parallel with the L-probe to simultaneously detect the expression of the L-mRNA$^{myc\text{-}zafA}$ and L-mRNA^{gfp} transcripts (Fig. 5B; Blot #2). In AF1043, both L-transcripts were detected 6 h after the zinc shock, whereas in AF1031, only the L-mRNA^{gfp} transcripts were constitutively detected, which showed that the expression of the L-mRNAs was ZafA-independent. To simultaneously detect the expression of the S- and L-mRNA^{gfp} transcripts, blot #2 was rehybridized with the GFP-probe (Fig. 5B; Blot#2^{R}). The expression level of S-mRNA^{gfp} transcripts reduced progressively in strain AF1043 after the zinc shock, whereas no S-mRNA^{gfp} transcripts were detected in AF1031. Instead, the previously detected signals for the L-mRNA^{gfp} transcripts intensified after hybridization with the GFP probe.

On the other hand, the amount of Myc-ZafA protein in AF1043 after zinc shock remained similar to the amount detected under zinc-limiting conditions for at least 20 min before it began to gradually decrease (Fig. 5C). The expression of the L-mRNA$^{myc\text{-}zafA}$ transcripts did not occur until most of the Myc-ZafA protein had disappeared, suggesting that Myc-ZafA repressed the expression of the L-mRNA$^{myc\text{-}zafA}$ transcripts, while it was inducing the expression of the S-mRNA$^{myc\text{-}zafA}$ transcripts. In addition, a small amount of Myc-ZafA, which was either recalcitrant to proteolytic processing or synthesized *de novo* upon the limited translation of the L-mRNA$^{myc\text{-}zafA}$ transcripts (due to the presence of several out-of-frame AUGs), was detected 6 h after the zinc shock (Fig. 5C). The GFP synthesized by AF1043 appeared to reflect the amount of S-mRNA^{gfp} transcribed following the zinc shock. However, the high stability of the GFP in fungi (Mateus and Avery, 2000) did not allow us to ascertain whether the GFP detected 6 h after the zinc shock had been synthesized *de novo.* The AF1031 mutant did not express the S-mRNA^{gfp} transcripts and, accordingly, did not synthesize a large amount of GFP. However, an exceedingly low signal was detected after overexposure as compared to the amount detected in AF1043 (Fig. 5C), indicating that the L-mRNA^{gfp} transcripts were being translated in AF1031 under both zinc-limiting and zinc-replete conditions. Finally, the basal amount of GFP synthesized constitutively by the Δ*zafA* AF1031 strain was similar to that produced by the wild-type AF1043 strain under sustained zinc-replete conditions (Fig. 5D), confirming the high stability of GFP in *Aspergillus.*

Taken together, these results showed that in a wild-type strain growing under zinc-limiting conditions ZafA induced the transcription of the S-mRNAs transcripts and simultaneously repressed the transcription of the L-mRNAs transcripts. In contrast, the transcription of the L-mRNAs occurred in a ZafA-independent manner, and their translation gave rise to a basal amount of ZafA under zinc-replete conditions.

Fig. 4. Transcription units of the *zafA* gene.

A. Total RNA was obtained from a wild-type strain (AF14) grown in SDN–Zn–Fe supplemented with the indicated increasing amounts of zinc and iron. RNA samples were long resolved in agarose-formaldehyde gels and analysed by Northern blot using two different probes (L and LS). The L-probe was a DNA fragment of 280 bp that was obtained by PCR using the pair of oligonucleotides JA124/JA204 as primers and, as template, a dilution of the plasmid pZAF48 (Moreno et al., 2007b). The LS-probe was a DNA fragment of 326 bp that was obtained by PCR using as primers the pair of oligonucleotides JA118/JA203 and, as template, the same dilution of the plasmid pZAF48. The L-probe hybridized between the nucleotide −315 and −594 pb upstream of the in-frame AUG codon whereas the LS-probe hybridized with a fragment located between the nucleotide −263 upstream of the in-frame AUG codon and + 63 downstream of this codon, as depicted in the scheme below the blots. Hence, we expected that the L-probe hybridized only with the L-transcripts, whereas the LS-probe should hybridize with both the L- and S-transcripts.

B. Schematic representation of the gDNA corresponding to the 5'-UTR of the *zafA* gene. To identify the TSSs of both transcripts, we used three different sets of primers (A, B and C) to synthesize 5′-phosphorylated cDNAs that were circularized, amplified by PCR and analysed as described in the material and methods section. The oligonucleotides for set A were JA428', JA429 and JA430); for set B were JA425', JA438 and JA439; and for set C were JA431', JA124 and JA432. Each set of primers included one 5′-phosphorylated primer (labelled with a prime and represented as green arrows) to synthesize a 5′-phosphorylated single stranded cDNAs. A pair of oligonucleotides of each set (represented as orange and black arrows) was used for PCR after recircularization of the cDNAs. Specifically, the set A of primers was used to identify the 5′-ends of the S-transcripts in the sample of RNA labelled with one asterisk (*) in panel A. The sets B and C of primers were used to identify the 5′-ends of the L-transcripts in the sample of RNA labelled with two asterisks (**) in panel A. The TSSs for the S-mRNA are indicated in the gDNA with black round lollipops. The TSSs for the LL-mRNA and SL-mRNA are indicated, respectively, in the gDNA with red and green rhomboid lollipops. The existence of two 5′-UTR intronic sequences (UIS1 and UIS2, in yellow) was confirmed by sequencing of a PCR fragment obtained using the pair of oligonucleotides JA203/JA394 (804 bp) as primers and, as template, cDNA synthesized from the sample of RNA labelled with two asterisks in panel A (**) using the oligonucleotide JA394 as primer.

C. Schematic representation of the different types of mature mRNAs produced by the transcript units of *zafA.* The in-frame AUG translation start codon is highlighted in green. The five out-of-frame AUG translation start codons are highlighted in light blue. The open triangulated lollipops indicate the exon-exon junctions in the mature mRNA. Notice that the S-mRNAs may have 6-7 exons but no out-of-frame AUG, whereas the L-mRNA may have 7-8 exons and 1-5 out-of-frame AUGs. [Color figure can be viewed at wileyonlinelibrary.com]

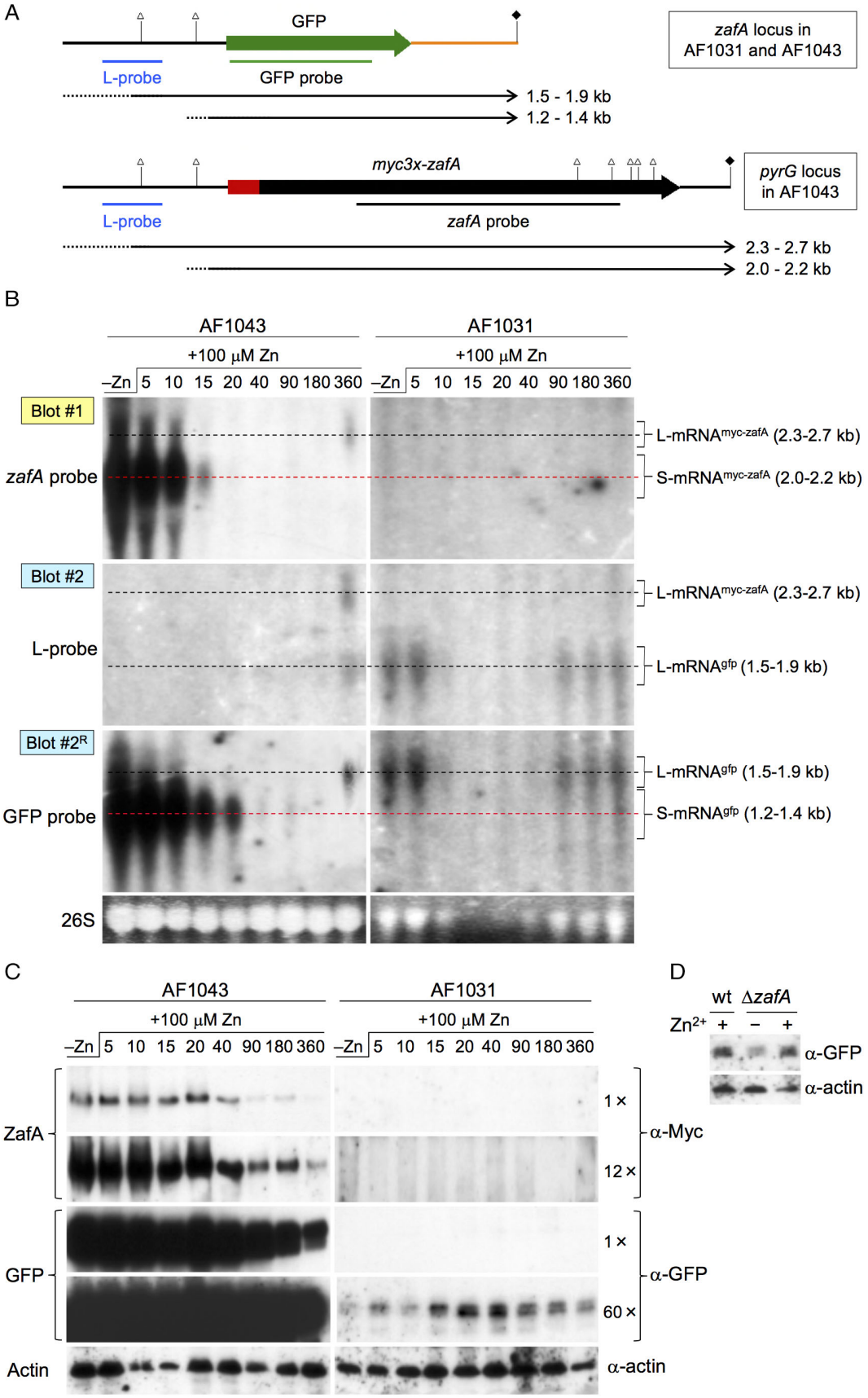
A
GFP
L-probe
GFP probe
1.5 - 1.9 kb
1.2 - 1.4 kb
zafA locus in AF1031 and AF1043
myc3x-zafA
L-probe
zafA probe
2.3 - 2.7 kb
2.0 - 2.2 kb
pyrG locus in AF1043
B
AF1043
AF1031
+100 μM Zn
–Zn 5 10 15 20 40 90 180 360
Blot #1
zafA probe
L-mRNAmyc-zafA (2.3-2.7 kb)
S-mRNAmyc-zafA (2.0-2.2 kb)
Blot #2
L-probe
L-mRNAmyc-zafA (2.3-2.7 kb)
L-mRNAgfp (1.5-1.9 kb)
Blot #2R
GFP probe
L-mRNAgfp (1.5-1.9 kb)
S-mRNAgfp (1.2-1.4 kb)
26S
C
AF1043
AF1031
+100 μM Zn
–Zn 5 10 15 20 40 90 180 360
ZafA
1 ×
12 ×
α-Myc
GFP
1 ×
60 ×
α-GFP
Actin
α-actin
D
wt
ΔzafA
Zn2+ + – +
α-GFP
α-actin

The transcription-activating function of ZafA is inhibited by zinc

The low environmental concentration of Zn^{2+} ions required to keep the expression of *zafA* completely off (between 4 and 10 μM zinc) (Fig. 3B), the relatively short lifespan (~20 min) of the mRNA transcripts of *zafA* (Fig. 5B) and of the other ZafA target genes (e.g. *zrfA* and *zrfB*) (Vicentefranqueira *et al.,* 2005), along with the presence of a relatively high amount of the ZafA protein in fungal cells between 10 and 180 min after a zinc shock (Fig. 5C), suggested that Zn^{2+} ions might inhibit the transcription-activating function of ZafA. In addition, ZafA has four putative zinc-binding domains in its N-terminus and a tCWCH2 motif that could bind several Zn^{2+} ions (Supporting Information Fig. S4). We hypothesized that ZafA, when saturated with Zn^{2+} ions, becomes transcriptionally inactive and susceptible to degradation. Hence, we anticipated that, for a fixed amount of ZafA, the higher the concentration of zinc in the medium, the more inactivation of ZafA. To investigate this, we constructed the AF1045 strain that constitutively synthesized the Myc-ZafA protein under the control of the promoter region of the actin gene (*actA*) from *Aspergillus nidulans* (Supporting Information Fig. S3), as described in the Experimental Procedures section. In the AF1043 strain, the expression of the S-mRNA$^{myc\text{-}zafA}$ transcripts was turned off at zinc concentrations higher than 3 μM. In the AF1045 strain, the *myc-zafA* coding sequence was expressed at similar levels in a broad range of zinc concentrations (Fig. 6A). Accordingly, in AF1043, the amount of Myc-ZafA reduced drastically in zinc-replete media, whereas in AF1045, the Myc-ZafA protein synthesized constitutively (Fig. 6B). The transcription of GFP (as a reporter of the Myc-ZafA activity on the expression of its own encoding gene) and *zrfC* (as a prototypic ZafA target gene) had been turned off in AF1045 in the presence of a relatively high amount of Myc-ZafA and a supplement of zinc ≥10 μM (Fig. 6A). This suggested that the transcription-activating activity of nearly all ZafA molecules had been inhibited in zinc-replete media. In agreement with the previous results, it would be expected that ZafA repressed L-mRNA expression in AF1045 under zinc-replete conditions. However, both the transcription profile and expression level of the L-mRNA^{gfp} transcripts in AF1045 were similar to those observed in AF1043, which suggested that ZafA saturated with Zn^{2+} ions might have suffered a conformational change that rendered it unable to enter the nucleus.

Zinc prevents that ZafA enters the nucleus under zinc-replete conditions

ZafA has a putative nuclear export signal (NES) located towards the N-terminus (Supporting Information Fig. S4), as predicted using LocNES (Xu *et al.,* 2015). Also, ZafA has a putative basic nuclear localization signal (NLS) located within the most C-terminal C2H2-type zinc finger (Supporting Information Fig. S4). We hypothesized that

Fig. 5. Regulation of the S- and L-mRNA expression at the transcriptional level.
A. Schematic representation of the S- and L-mRNAs encoding the green fluorescent protein (GFP) (in both the wild-type AF1043 and the Δ*zafA* mutant AF1031 strain) and the Myc-ZafA transcription factor in AF1043. The sequence of the 5'-UTRs of the S- and L-mRNAs in AF1043 and AF1031 were identical to that of the AF14 wild-type strain. The zafA coding sequence in AF1043 and AF1031 had been replaced precisely by that of the GFP (green arrow) followed by the terminator-polyadenylation signal of the An12g03580 gene from Aspergillus niger (in orange). The Myc3×–tag coding sequence (in red) was fused to the 5′-end of the *zafA* coding sequence (black arrow). The exon-exon junctions in the mature mRNAs are indicated by open triangulated lollipops. The estimated sizes of the S- and L-mRNA^{gfp} were between 1.2-1.4 and 1.5-1.9 kb, respectively. The estimated sizes of the S- and L-mRNA$^{myc\text{-}zafA}$ were between 2.0-2.2 and 2.3-2.7 kb (including the sequence encoding the Myc3×–tag), respectively.
B. Analysis by Northern blot of the S- to L-mRNA transcriptional shift. The strains were grown in the SDN–Zn–Fe medium supplemented with 6 μM Fe for 20 h before applying a zinc shock with 100 μM zinc. Culture samples were taken at the indicated time periods (in minutes) after the zinc shock. The samples of mycelium were used to obtain both RNA and protein extracts. The RNA samples were transferred by duplicate onto nylon membranes. One was hybridized with the zafA probe (Blot#1). The other one was hybridized with the L-probe (Blot#2) and later with the GFP probe (Blot#2R). The DNA fragment used as a probe for sGFP was obtained by PCR using the oligonucleotide pair JA502/qSGFP-R (556 bp) as primers and a diluted aliquot of the plasmid pMCB32 as template (Fernández-Ábalos et al., 1998). It was consistently observed that the samples of mycelia from the AF1031 strain corresponding to 10-40 min contained an extremely low amount of RNA compared to other time points. Nevertheless, these samples were included in the gel for consistency with the blots shown for AF1043. Hence, if L-mRNA transcripts were not detected in the AF1031 strain between 10 and 40 min was because the amount of total RNA after the zinc shock was transiently reduced (as revealed the low amount of 26S rRNA). In addition, this finding suggested that the adaptive response displayed by the Δ*zafA* strain to deal with a sudden zinc-replete condition involved a broad transcriptional and translational readjustment that even affected ribosome biosynthesis, and that ZafA was required not only to adapt fungal growth to zinc-limiting conditions but also to zinc-replete conditions since a Δ*zafA* mutant takes longer than a wild-type (about 30 min) to adapt to zinc-replete conditions.
C. Protein extracts were prepared from the same mycelium samples used to obtain total RNA. Proteins were analysed by Western blot using specific antibodies against the c-myc epitope and GFP to detect Myc-ZafA and sGFP, respectively. For each blot, two different exposure times were shown, and the relative exposure times during their development have been indicated on their right for comparison purposes (a 1× relative exposure time equals to an exposure for 30 s).
D. The wild-type AF1043 and the Δ*zafA* mutant AF1031 strain were grown in SDN–Zn–Fe medium supplemented with 6 μM Fe and ± 100 μM zinc as indicated. The synthesis of GFP was analysed by Western blot. [Color figure can be viewed at wileyonlinelibrary.com]

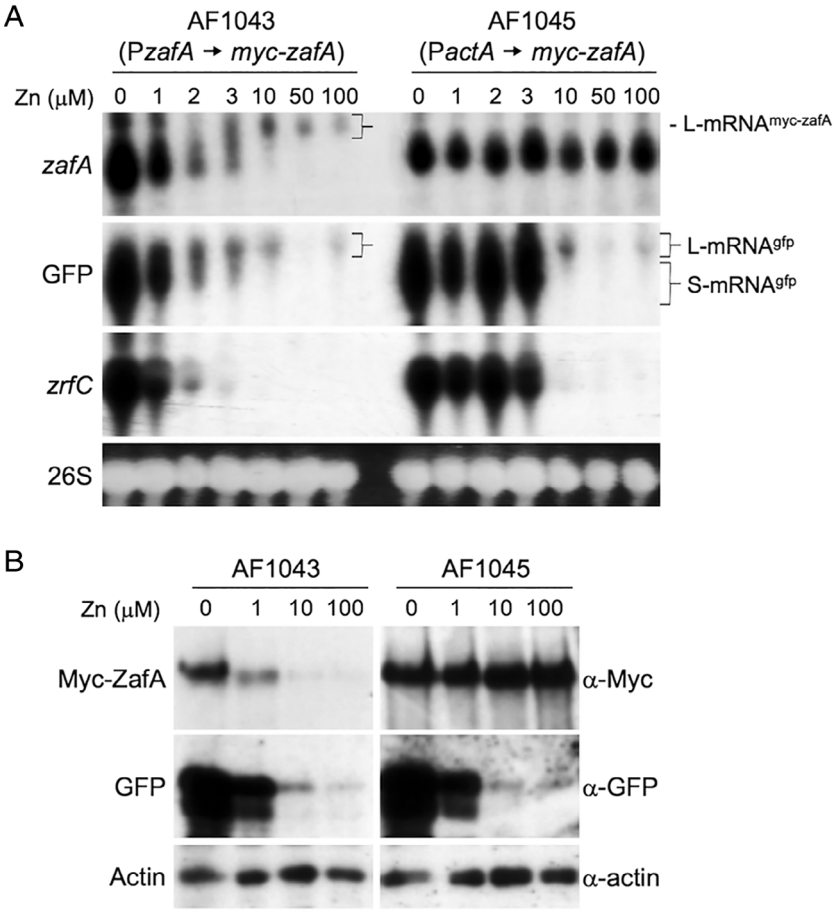

Fig. 6. Zinc inhibits the transcription-activating function of ZafA.
A. The AF1043 and AF1045 strains were grown in SDN–Zn–Fe medium supplemented 6.0 μM iron and increasing amounts of zinc, as indicated. Total RNA was obtained and analysed by Northern blot using the same DNA fragments used as probes for *zafA* and GFP. A DNA fragment of 804 bp obtained by PCR using the oligonucleotide pair JA60/JA294 and a diluted aliquot of the plasmid pZRF30 carrying the cDNA of *zrfC* (Amich et al., 2010) was used as a probe for *zrfC.*
B. Protein extracts were obtained from the same samples of mycelium that had been used to obtain total RNA, which were grown in media supplemented only with 1, 10 and 100 μM zinc. Proteins were analysed by Western blot using specific antibodies against the c-myc epitope and GFP to detect Myc-ZafA and sGFP, respectively.

most of the basal amount of ZafA detected under zinc-replete conditions was located either in the cytoplasm or moved continuously back and forth between the cytoplasm and the nucleus. Thus, when the concentration of Zn^{2+} in the cytoplasm dropped below a certain threshold, the migration of ZafA from the cytoplasm into the nucleus or the block of the ZafA movement between the nucleus and the cytoplasm would be triggered. Either event would result in the nuclear retention of ZafA. To investigate whether the environmental concentration of zinc influenced the subcellular location of ZafA, we constructed a *zafA*-reconstituted strain that expresses a GFP-tagged version of ZafA in the *zafA* locus (AF1047) under the control of the wild-type [AFUA_1G10060‑ AFUA_1G10080/*zafA*] intergenic sequence harbouring both the 5′-UTRs of the *zafA* transcripts and the *zafA* promoter region (Supporting Information Fig. S5). We clearly observed a fluorescent signal in the nucleus of hyphae cultured in zinc-limiting media (Fig. 7). In contrast, the GFP-ZafA protein appeared distributed throughout the cytoplasm and excluded from the nuclei under zinc-replete conditions. This indicated that the basal amount of ZafA synthesized under zinc-replete conditions was located in the cytoplasm rather than being moved continuously back and forth between the cytoplasm and the nucleus.

Iron availability determines the basal amount of ZafA that is synthesized under zinc-replete conditions by differentially regulating the expression level of the LL- and SL-mRNA transcripts

To determine in detail the effect of iron on the expression of the different *zafA* transcripts, we cultured the AF1043 and AF1031 strains in a zinc-replete media supplemented with increasing amounts of iron and quantified the relative expression levels (REL) of all *zafA* (LL-/SL-/S-mRNA$^{myc\text{-}zafA}$) and/or GFP transcripts (LL-/SL-/S-mRNA^{gfp}) (as reporters of the Myc-ZafA function) by RT-qPCR (Fig. 8A). In the AF1043 strain grown in zinc-replete media, both the REL and percentage of the LL-mRNA$^{myc\text{-}zafA}$ and LL-mRNA^{gfp} transcripts lowered with the iron supplement and increased those of their corresponding SL/S-mRNA$^{myc\text{-}zafA}$ and SL/S-mRNA^{gfp} transcripts, while keeping constant the LL^{gfp}:LL$^{myc\text{-}zafA}$, SL^{gfp}:SL$^{myc\text{-}zafA}$ and S^{gfp}:S$^{myc\text{-}zafA}$ ratios. As expected,

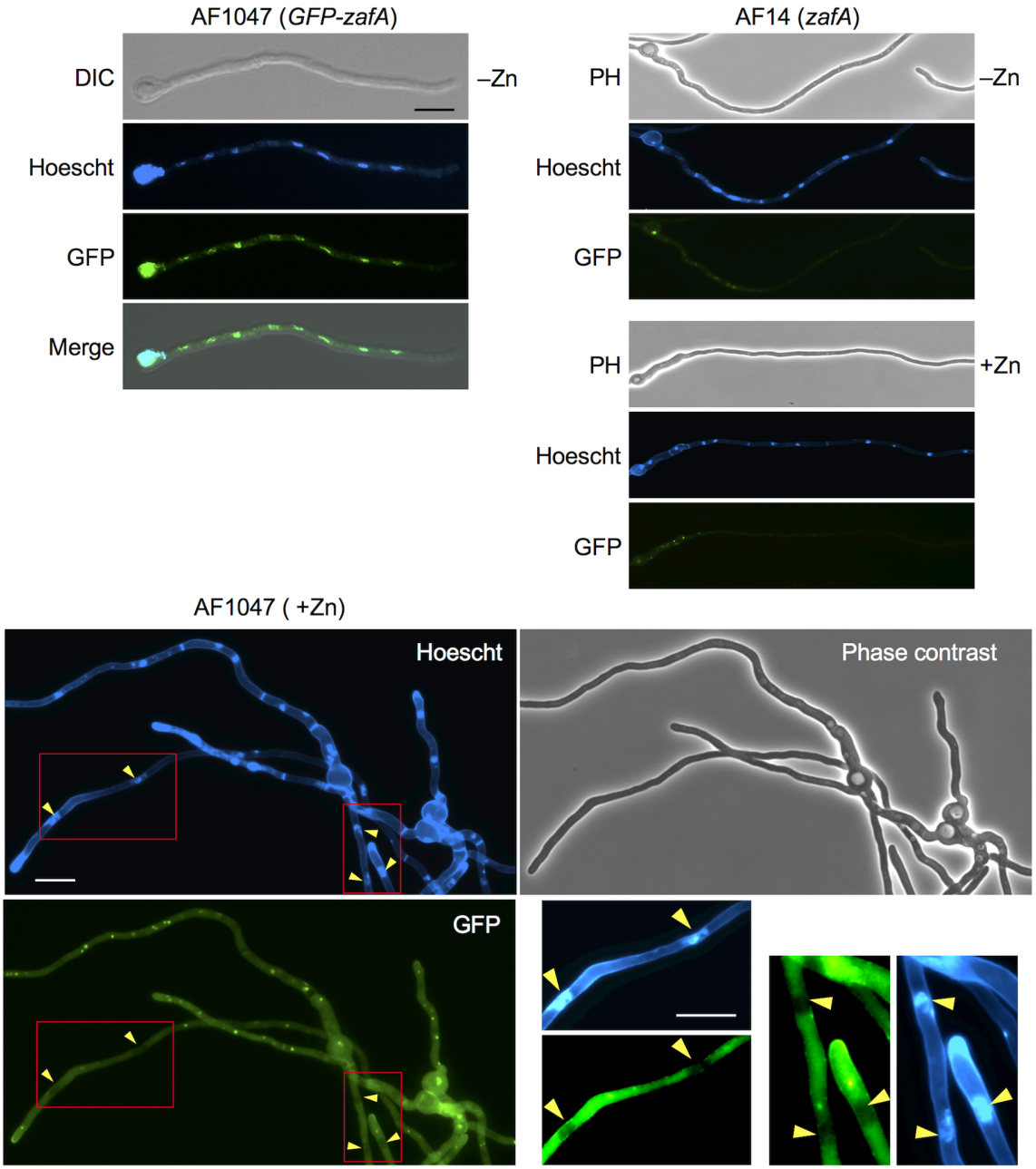

Fig. 7. Subcellular location of ZafA in response to the environmental concentration of zinc. A modified version of the *Aspergillus* minimal medium (A3M) was used as the culture medium to prevent the precipitation of metallic salts in fungal cultures used for fluorescence microscopy. Approximately 5×10^5 conidia of both the AF14 (expressed a wild type, non-tagged ZafA protein) and AF1047 strain (expressed a wild type, GFP-tagged ZafA protein) were inoculated into 0.5 ml of the A3M medium without a zinc supplement (–Zn) or supplemented with 5 μM zinc (+Zn), dispensed in wells of a 24-multiwell plate and incubated for 18 h at 28°C without shaking. Germlings were deposited onto a coverslip containing 5 μl of Hoeschst 33,258 (1 mg/ml). The coverslip was flipped onto one slide, incubated at room temperature for 10 min and was observed using a Leica DMRXA epifluorescence microscope equipped with a 63×/1.4 oil plan-apochromat objective and a DFC350FX camera. The time of exposition was 20 s for GFP and 0.1 s for Hoechst. The images that were taken corresponded to the first exposure to the excitation light. All images were taken using the same exposure and microscope settings. The AF14 wild-type strain was used as a reference to determine the right settings in order to avoid non-specific background noise. Scale bars, 5 μm. [Color figure can be viewed at wileyonlinelibrary.com]

the Δ*zafA* AF1031 strain did not synthesize S-mRNA^{gfp} transcripts under zinc-limiting conditions (Fig. 8A). In zinc-limiting media, the relative expression ratio (rER) of the LL- and SL-mRNA^{gfp} transcripts synthesized by AF1031 was >20-fold higher than those synthesized by the AF1043 strain (Fig. 8B), which was consistent with the ZafA-mediated repression of L-mRNA transcripts in a wild-type strain under zinc-limiting conditions. In zinc-

replete media supplemented with 6 μM iron, the rER of the LL-mRNA^{gfp} transcripts in AF1031 was similar to that in AF1043, whereas the rER of the SL-mRNA^{gfp} transcripts was about 20-fold lower in AF1031 than in AF1043 (Fig. 8B). In zinc- and iron-replete media, the rER of the LL-mRNA^{gfp} transcripts in AF1031 was >25-fold higher than in AF1043, whereas the rER of the SL-mRNA^{gfp} transcripts in AF1031 was similar to that in AF1043. We took advantage of the high stability of GFP (compared to that of ZafA) to detect low levels of L-mRNA translation in these strains (Fig. 8C). The amount of GFP synthesized under zinc-replete conditions in AF1031, compared to that in AF1043, appeared to reflect the rER of the SL-mRNA^{gfp} transcripts in AF1031 with respect to AF1043. This result was also consistent with the lower number of out-of-frame AUGs in the SL-mRNA^{gfp} than in the LL-mRNA^{gfp} transcripts. Intriguingly, this finding also indicated that the lack of ZafA completely repressed the expression of the SL-mRNA^{gfp} transcripts under zinc-replete, iron-limiting conditions.

To confirm whether the basal amount of GFP increased with the iron supplement under zinc-replete conditions, we analysed the synthesis of GFP in the AF1043 strain grown in zinc- and iron-limiting medium supplemented with increasing amounts of zinc and iron (Fig. 8D). In agreement with our prediction, the highest

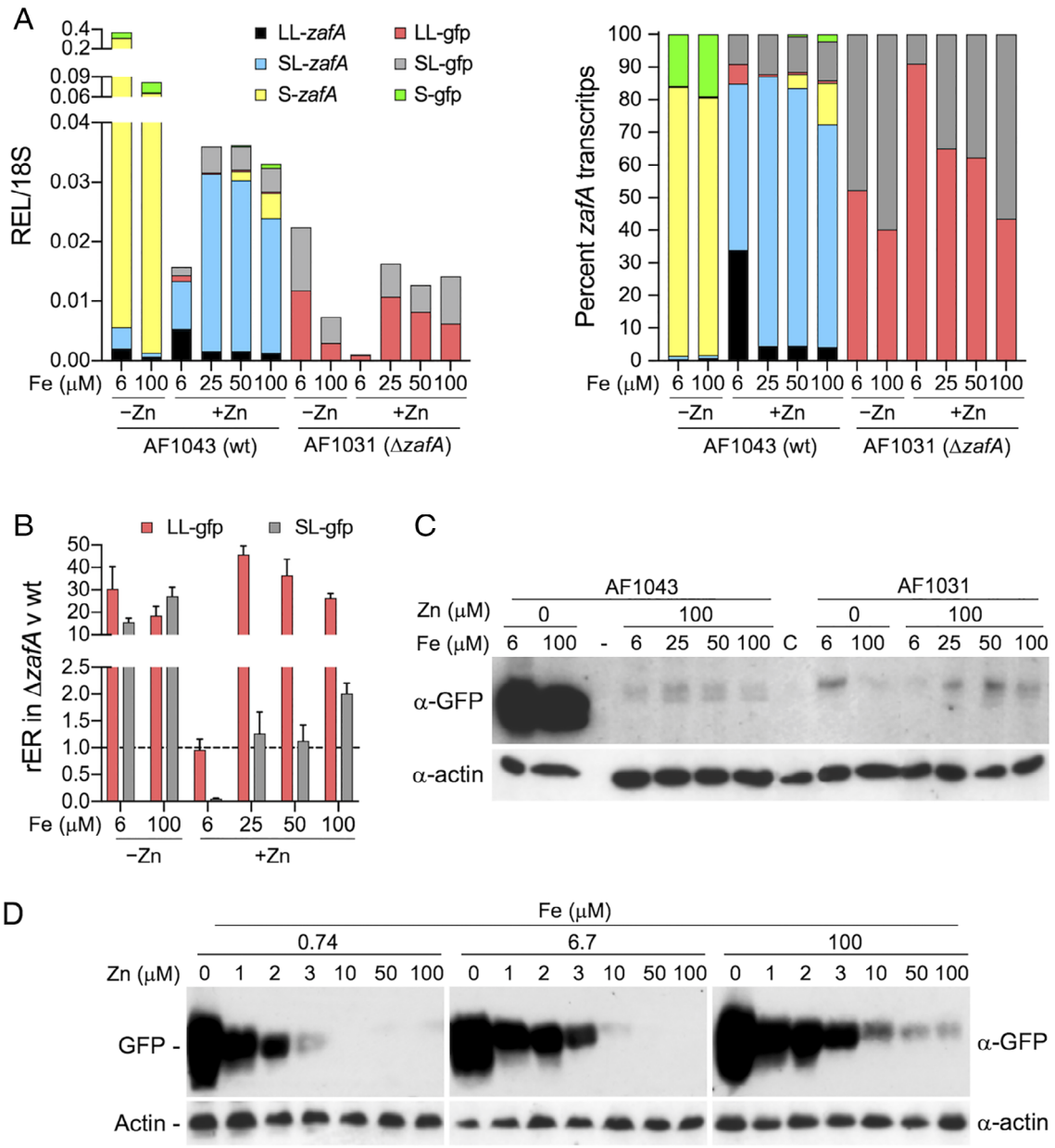

amount of GFP was detected in media supplemented with the highest iron concentration tested (i.e., 100 μM Fe) (Fig. 8D) under zinc-replete conditions (≥10 μM Zn).

Taken together, these results suggested that L-mRNA repression under zinc-limiting conditions was ZafA dependent, regardless of iron availability. In contrast, LL-mRNA and SL-mRNA expression in zinc-replete media appeared to be differentially regulated by iron availability, such that the strongest LL-mRNA induction (and SL-mRNA repression) occurred under iron-limiting conditions leading to an extremely low biosynthesis level of the basal amount of ZafA. In contrast, the strongest LL-mRNA repression (and SL-mRNA induction) occurred under iron-replete conditions allowing a relatively higher biosynthesis level of the basal amount of ZafA. Last, these results suggested that either the LL-mRNA induction or SL-mRNA repression under zinc-replete, iron-limiting conditions should be mediated by an iron-responsiveness factor whose expression and/or activity are positively influenced by iron starvation and/or zinc excess.

The transcription regulatory activity of ZafA and HapX appears to be modulated by the intracellular Zn:Fe ratio

It was previously shown that the expression of genes *hapX* and *srbA*, which encode factors involved in the regulation of iron homeostasis, was down-regulated under zinc-limiting, iron-replete conditions (Vicentefranqueira *et al.,* 2018). To investigate whether an excess of zinc influenced the expression and/or function of these regulators in addition to that of ZafA, we created a fungal strain (AF1059) that expressed *zrfC* in zinc-replete media under the control of the promoter of the *actA* gene from *A. nidulans* [P*actA* → *zrfC*] (Supporting Information Fig. S6). The REL of *zrfC*, which encodes the major zinc transporter of *A. fumigatus* required for zinc uptake from alkaline zinc-limiting media (Amich *et al.,* 2010), was not influenced by iron availability in AF1059 grown in alkaline zinc-replete media (Supporting Information Fig. S6C, left panel). However, the basal REL of *zrfC* in the wild-type strain (AF14) grown in zinc-replete media was noticeably influenced by iron, such that it was about 5-fold higher under iron-replete conditions (i.e., in media supplemented with ≥25 μM iron) than under iron-limiting conditions (i.e., in media supplemented with ≤6 μM iron) (Supporting Information Fig. S6C, left panel). This indicated that the relative expression ratio (rER) of *zrfC* in AF1059 was on average between 35-fold and 140-fold higher than in AF14 grown in iron-replete and iron-limiting media, respectively (Supporting Information Fig. S6C, right panel). Hence, it would be expected that (i) the intracellular Zn:Fe ratio in AF1059 grown in zinc-replete media is higher under iron-limiting than under iron-replete conditions and (ii) the AF1059 strain grown in zinc-replete media contains a higher amount of intracellular zinc than the wild-type strain. Thus, we cultured both the AF14 and AF1059 strains in zinc-replete media supplemented with increasing amounts of iron. Then the REL, the percentages and rER of the different *zafA* transcripts (LL-/SL-/S-mRNA) were measured by RT-qPCR as described in the Experimental Procedures section (Supporting Information Fig. S7A). Interestingly, in AF1059, the rER of the LL-mRNA transcripts increased, while those of the SL- and S-mRNA transcripts reduced in the presence of the iron supplement. Accordingly, the rER of direct ZafA target genes, such as *zrfB*, *zrfC* and *zrcA*, changed as would be expected if the intracellular amount of zinc were high

Fig. 8. Regulation by iron of the basal amount of ZafA that is synthesized under zinc-replete conditions.
A. The AF1043 and AF1031 strains were grown in the SDN–Zn–Fe medium supplemented with zinc and increasing amounts of iron, as indicated. RNA was analysed by RT-qPCR, as described in the experimental procedures section, to measure the relative expression level (REL) of all *myc-zafA* and/or GFP transcripts (LL-/SL-/S-mRNA$^{myc\text{-}zafA}$ and LL-/SL-/S-mRNA^{gfp}) using the 18S rRNA as an internal reference (REL/18S) (left graph), and the percentage of each type of mRNA in every sample tested (right graph). Notice that the AF1043 strain carried both the *myc-zafA* and GFP coding sequences whereas the Δ*zafA* AF1031 strain only carried the GFP coding sequence, all of them under the control of the *zafA* promoter. Although in the AF1043 strain, the amount of LL-, SL-and S-mRNA should be theoretically identical for GFP and zafA, they were not, most likely due to differences in mRNA stability and/or the loci in which these genes are expressed. It must be noted that in the AF1043 strain the relative amount of all *zafA* transcripts were about 6.3-fold more abundant than that of the GFP transcripts under zinc-replete conditions (4.7-fold under zinc-limiting conditions). In addition, the relative amount of GFP transcripts in AF1043 under zinc-limiting conditions (regardless of the iron supplement) and in a zinc-replete medium supplemented with 6 μM iron was 2.5-fold higher than in the AF1031 strain. In contrast, in media supplemented with ≥25 μM iron, the relative amount of GFP transcripts in AF1043 was about 2.9-fold lower than in the AF1031 strain. In either case, the extremely high stability of GFP compared to that of Myc-ZafA appeared to compensate the relatively lower amount of GFP transcripts. RT-qPCR results are the average of two biological replicates. Error bars have been omitted to gain clarity for data representation in stacked columns.
B. The relative expression ratio (rER) of the LL-/SL-mRNA^{gfp} in AF1031 (Δ*zafA*) compared to AF1043 (wt) was calculated from the same RT-qPCR data shown in part A, as described in the experimental procedures section.
C. Analysis by Western blot of the basal amount of GFP that is found in proteins extracts obtained from the same samples used to obtain RNA samples. The sample labelled as C (for background control) referred to a protein sample obtained from the wild-type strain AF14 (that did not carry any GFP-tagged protein) grown under zinc- and iron-replete conditions.
D. The AF1043 strain was grown in the SDN–Zn–Fe medium supplemented with iron and increasing amounts of zinc, as indicated. Mycelia were used to prepare proteins extracts that were analysed by Western blot using an anti-GFP antibody. All blots were processed and developed simultaneously with increasing exposure times. The blots presented in the figure have not been overexposed to better show the differences among them. [Color figure can be viewed at wileyonlinelibrary.com]

enough so as to inhibit the transcription regulatory activity of the basal amount of ZafA (i.e., *zrfB* and *zrfC* expression reduced while that of *zrcA* increased), being this inhibition greater under iron-replete than under iron-limiting conditions (Supporting Information Fig. S7B). If an intracellular excess of zinc influenced the transcription regulatory activity of HapX and/or SrbA, the expression profile of their most direct target genes (including their own encoding genes) should be readjusted in AF1059. An intracellular excess of zinc did not noticeably influence the rER of *srbA* in zinc-replete media, neither under iron-limiting nor iron-replete conditions. Similarly, it did not influence the rER of *hapX* under zinc-replete, iron-limiting conditions, although it was found to be reduced by 2-fold under zinc- and iron-replete conditions (Supporting Information Fig. S7B). The rER of *mirB* (induced by HapX) and *hemA* (repressed by HapX), as reporters of HapX activity (Schrettl *et al.,* 2010), changed accordingly in the AF1059 strain (Supporting Information Fig. S7B). It was noteworthy that an intracellular excess of zinc under zinc- and iron-replete conditions caused both the down-regulation of *hapX* and a reduction in the rER of the SL- and S-mRNA transcripts (coupled to up-regulation of LL-mRNA transcripts). Taken together, these results suggested that the transcription regulatory activity of both HapX and ZafA could be influenced directly by zinc and/or iron depending on the intracellular Zn:Fe ratio.

Moreover, the rER of the different *zafA* transcripts in a Δ*sreA* mutant (Supporting Information Fig. S7C) were measured to determine any putative effect caused by an intracellular excess of iron on ZafA activity. It would be expected that the intracellular amount of iron in this mutant grown in a medium non-supplemented with iron is similar to that in its parental wild-type strain (CEA10), whereas the intracellular amount of iron would increase in a Δ*sreA* mutant when grown in media supplemented with iron (Schrettl *et al.,* 2008). Hence, the intracellular Zn:Fe ratio in the Δ*sreA* mutant grown in a zinc-replete medium non-supplemented with iron should be higher than in a medium supplemented with ≥6 μM iron. The rER of the SL- and S-transcripts in the Δ*sreA* mutant increased in a zinc-replete medium supplemented with 6 μM iron as compared to a wild-type strain (Supporting Information Fig. S7C). Actually, the 4-fold increase of the S-mRNA could explain the up-regulation of *zrfC* and the down-regulation of *zrcA* under this culture condition (Supporting Information Fig. S7D). Moreover, the expression profile of these genes suggested that zinc taken up from the medium supplemented with 6 μM iron was used for fungal growth rather than being stored to prevent its toxicity. In addition, it is known that the expression of *hapX*, *mirB* and *ftrA* is repressed by SreA (Schrettl *et al.,* 2010; Blatzer *et al.,* 2011). Indeed, the rER of these genes in a Δ*sreA* mutant increased noticeably under iron-replete conditions compared to a wild-type strain, which indicated that an intracellular iron excess enhanced HapX activity in zinc-replete media (Supporting Information Fig. S7D). However, the rER of *hapX* in the Δ*sreA* mutant grown in a zinc-replete medium was unexpectedly reduced by 2-fold under iron-limiting conditions. This could nevertheless indicate that the intracellular Zn:Fe ratio in the Δ*sreA* mutant under these culture conditions resembled the intracellular Zn:Fe ratio in AF1059 grown under zinc- and iron-replete conditions. In this regard, it is remarkable that the percentage of the different *zafA* transcripts in AF1059 under iron-replete conditions (Supporting Information Fig. S7A) resembled that found in the Δ*sreA* mutant grown in a medium non-supplemented with iron (Supporting Information Fig. S7C). Taken together, these results were consistent with the notion that the intracellular Zn:Fe ratio modulated in some way the transcription regulatory activity of both HapX and ZafA.

The expression of the L-mRNA transcripts in zinc-replete media is regulated by HapX under both iron-replete and iron-limiting conditions

The LL-transcripts expressed chiefly under zinc-replete, iron-limiting conditions, whereas the SL-transcripts expressed predominately under zinc- and iron-replete media (Fig. 4). Hence, the expression profile of the L-transcripts resembled what would be expected, if their transcription was regulated by iron availability. It was previously shown that the major transcription factors involved in the regulation of iron homeostasis were SreA, HapX, SrbA and SrbB (Schrettl *et al.,* 2008; Schrettl *et al.,* 2010; Blatzer *et al.,* 2011; Chung *et al.,* 2014). To ascertain whether any of these regulators of iron homeostasis modulated zinc homeostasis, we cultured the Δ*sreA*, Δ*hapX*, Δ*srbA* and Δ*srbB* mutant strains onto zinc- and iron-limiting agar media with and without the iron chelator BPS to provide, respectively, harsh and mild iron-limiting conditions (Supporting Information Fig. S8A). The growth ability of the Δ*srbA* and Δ*srbB* mutants on BPS-containing plates became fully restored as the zinc supplement increased, whereas that of the Δ*hapX* strain was only partially restored. This indicated that *srbA* and *srbB* were required for fungal growth in zinc-limiting media under harsh iron-limiting conditions whereas *hapX* was required for a healthy fungal growth in iron-limiting media under both zinc-limiting and zinc-replete conditions. Therefore, we measured the net growth of this strain in a liquid media free of chelators to more accurately determine the effect of zinc on the growth ability of a Δ*hapX* mutant, depending on iron availability (Supporting Information Fig. S8B). The growth ability of a

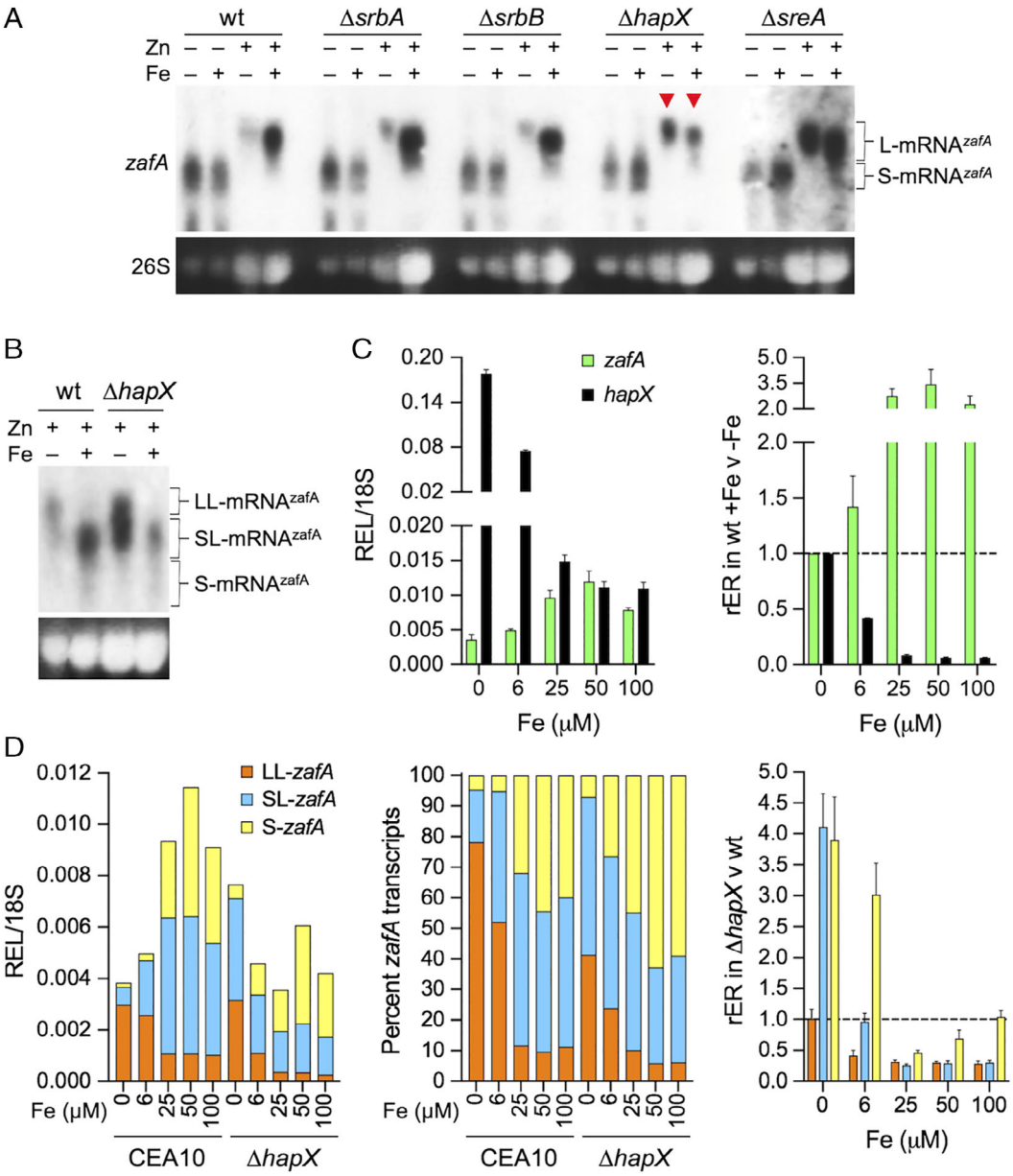

Fig. 9. Effect of HapX on the regulation of zinc homeostasis in zinc-replete media depending on iron availability.

A. Total RNA was obtained from CEA10 (wt) and the Δ*srbA*, Δ*srbB*, Δ*hapX* and Δ*sreA* mutant strains grown in the SDN–Zn–Fe medium with or without a supplement of 100 μM zinc and/or 50 μM iron. RNA was analysed by Northern blot. We loaded in the gel an amount of total RNA obtained from the fungal strains grown under zinc-replete conditions that was approximately 20-fold higher than that obtained from the fungal strains grown under zinc-limiting conditions in order to improve the detection of the L-transcripts and to prevent that the strong signal of the S-mRNA transcripts detected under zinc-limiting conditions covered up the weak signals of the L-mRNA transcripts detected under zinc-replete conditions. A 1038-bp DNA fragment of the *zafA* coding sequence, which was obtained by PCR as described in figure legend 2, was used as a probe to detect all *zafA* transcripts.

B. RNA samples from both the wild-type and Δ*hapX* mutant strain grown under zinc-replete conditions were loaded side by side, separated in a long-resolved formaldehyde gel and reanalysed by Northern blot using the same *zafA* probe.

C. Total RNA was obtained from the CEA10 strain grown in the SDN–Zn–Fe medium supplemented with 100 μM zinc and increasing amounts of iron, as indicated. RNA analysed by RT-qPCR to measure the relative expression level (REL) and the relative expression ratio (rER) of total *zafA* transcripts and *hapX*, with respect to that found in the wild-type strain grown in medium non-supplemented with iron. The oligonucleotides used to quantify expression by RT-qPCR were ZAFA-D5/ZAFA-R5 (for *zafA*) and HAPX4-D/HAPX3-R (for *hapX*).

D. Total RNA was obtained from the CEA10 strain and Δ*hapX* mutant grown in the SDN–Zn–Fe medium supplemented with 100 μM zinc and increasing amounts of iron as indicated. RNA that was analysed by RT-qPCR to measure the REL, the percentage and the rER of the different types of *zafA* transcripts in the Δ*hapX* mutant, with respect to that found in the wild-type strain. RT-qPCR results are the average of two biological replicates. Error bars indicate standard deviation (omitted to gain clarity for data representation in the stacked columns). [Color figure can be viewed at wileyonlinelibrary.com]

wild-type strain was higher in an iron-limiting medium supplemented with 10 μM zinc than with 100 μM Zn. This negative effect of zinc on fungal growth under iron-limiting conditions was significantly enhanced in the absence of *hapX.* Importantly, this finding suggested that HapX could play a role in regulating *zafA* expression under zinc-replete, iron-limiting conditions, which is in agreement with previous results reported by other investigators (Schrettl *et al.,* 2010).

In either case, to ascertain the putative role of the major regulators of iron homeostasis on *zafA* transcription, we analysed the expression of *zafA* by Northern blot in the Δ*sreA*, Δ*hapX*, Δ*srbA* and Δ*srbB* mutant strains (Fig. 9A). Interestingly, the most noticeable change in the expression profile of *zafA* compared to a wild-type strain pertained to the L-mRNA transcripts detected in the Δ*hapX* mutant grown under zinc-replete conditions. In order to better separate the different types of L-mRNA transcripts in the Δ*hapX* strain grown under zinc-replete conditions, we reanalysed, side by side, the samples of RNA from both the Δ*hapX* and wild-type strain in a long-resolved gel (Fig. 9B). Thus, it was shown that the amount of the SL-transcripts in the Δ*hapX* strain grown in zinc-replete media under iron-replete conditions was lower than in a wild-type strain. In addition, under zinc-replete, iron-limiting conditions, both the LL- and SL-mRNA transcripts were readily detected in the Δ*hapX* strain at a level higher than in the wild type (Fig. 9B). We confirmed that the expression level of *hapX* and *zafA* in a wild-type strain grown under zinc-replete conditions exhibited opposite expression profiles, where the expression of *zafA* increased as the expression of *hapX* decreased with the iron supplement, as shown by RT-qPCR (Fig. 9C).

To determine in detail the effect of HapX on the expression of the different types of *zafA* transcripts, depending on the iron content of the media, we cultured the Δ*hapX* strain in zinc-replete media supplemented with increasing amounts of iron. Both the REL and relative expression ratios (rER) of the different *zafA* transcripts compared to that in the wild-type strain were then measured by RT-qPCR (Fig. 9D). In the Δ*hapX* mutant, grown in media without an iron supplement, the rER of the LL-mRNA was similar to that found in a wild type strain, whereas the rER of both the SL- and S-mRNA was >3.5-fold higher than in the wild type. In contrast, the rER of all *zafA* transcripts in the Δ*hapX* mutant reduced, compared to the wild type, as increased the iron supplement (Fig. 9D, right panel). Furthermore, it was remarkable that the percentage of the LL-, SL- and S-mRNA transcripts differed between the wild type and Δ*hapX* mutant in zinc-replete media under iron-limiting conditions, such that the LL-mRNA transcripts predominated over the SL-mRNA transcripts (Fig. 9D, middle panel). Taken together, these results strongly suggested that in a wild-type strain grown under zinc-replete, iron-limiting conditions, HapX repressed the expression of the SL/S-mRNA transcripts, while allowing the expression of the LL-mRNA transcripts. In contrast, under zinc- and iron-replete conditions, HapX enhanced the expression of the SL-mRNA transcripts, while repressing the expression of the LL-mRNA transcripts.

Discussion

During our initial studies on the regulation of zinc homeostasis by ZafA (Moreno *et al.*, 2007b), we realized that the net fungal growth of a Δ*zafA* mutant differed noticeably from that of wild type depending on the amount of zinc and iron in the media. This led us to suspect the existence of a putative co-regulatory network for Zn/Fe homeostasis.

It is known that HapX, SrbA, SrbB and the SreA GATA factor are major regulators of iron homeostasis in *A. fumigatus* (Schrettl *et al.,* 2008; Schrettl *et al.,* 2010; Blatzer *et al.,* 2011; Chung *et al.,* 2014). Under zinc-replete, iron-limiting conditions, HapX represses *sreA* and genes encoding iron-requiring proteins, and at the same time up-regulates the expression of genes encoding proteins for iron uptake in addition to its own encoding gene (Schrettl *et al.,* 2010; Gsaller *et al.,* 2014). SrbA, on the other hand, induces *hapX* and genes encoding proteins involved in iron uptake and non-haem iron-requiring enzymes involved in ergosterol biosynthesis (Blatzer *et al.,* 2011). In contrast, under zinc- and iron-replete conditions, SreA represses *hapX* and genes encoding proteins involved in iron acquisition (Schrettl *et al.,* 2010). SrbA and SrbB induce the expression of their own encoding genes during hypoxia and that of others encoding proteins involved in ergosterol biosynthesis or iron uptake, even under iron-replete conditions (Chung *et al.,* 2014). Evidence regarding the existence of a Zn/Fe interplay based on the transcriptional profiling studies of the Δ*hapX*, Δ*srbA*, Δ*srbB* and Δ*sreA* mutants was found during the analysis of the role of HapX, SrbA, SrbB and SreA on iron homeostasis in *A. fumigatus.* (Schrettl *et al.,* 2008; Schrettl *et al.,* 2010; Chung *et al.,* 2014). After a shift of a wild-type strain and a Δ*sreA* mutant from iron-limiting to iron-replete conditions, the expression level of the zinc homeostatic genes *zafA* and *zrfB* was up-regulated, whereas that of *zrcA* was down-regulated (Schrettl *et al.,* 2008), However, the expression level of these genes remained largely unchanged in a Δ*hapX* mutant after a shift from iron-limiting to iron-replete conditions (Schrettl *et al.,* 2010). This suggested that HapX repressed either directly or indirectly the expression of *zafA* and *zrfB*, while it induced either directly or indirectly the expression of *zrcA.* On the other

hand, after the shift of a wild-type strain from normoxic to hypoxic conditions in zinc- and iron-replete media, the expression level of several zinc homeostatic genes, such as *zrfA*, *zrfB*, *zrfC*, *zrfF*, *zrcA* and *zrcC*, was up-regulated, whereas that of *zafA* was down-regulated compared to a Δ*srbA* mutant (Chung *et al.,* 2014). Similarly, the expression of the *zrfA*, *zrfB* and *zrfC* was up-regulated, whereas that of *zafA*, *zrfF*, *zrcA* and *zrcC* was down-regulated compared to a Δ*srbB* mutant (Chung *et al.,* 2014). Unlike all previous studies carried out under zinc-replete conditions, we have recently shown that expression of *hapX*, *srbA* and *srbB* and that of several genes encoding proteins involved in iron-uptake and ergosterol biosynthesis was down-regulated in zinc-limiting media under iron-replete conditions (Vicentefranqueira *et al.,* 2018). In summary, all previous findings strongly suggested the existence of an interconnection between the regulation of iron and zinc homeostasis, which caused us to contemplate how iron availability influences *zafA* expression and/or modulated ZafA function even under zinc-replete conditions.

The main discovery that led us to investigate the interplay between iron and zinc homeostasis was that *zafA* had different transcription units that gave rise to different transcripts in zinc-replete media depending on iron availability. This finding was of interest as it could explain the underlying mechanism to determine the basal amount of ZafA that is synthesized under zinc-replete conditions. Actually, this is what would be expected if ZafA also functioned as an intracellular zinc sensor, the same as the Zap1 transcription factor in *S. cerevisiae* (Zhao and Eide, 1997) and explains the inhibition of the ZafA transcription-activating function by zinc. Although the N-terminus of Zap1 from *S. cerevisiae* is very different from that of ZafA, they both have a high number of Cys and His residues. Most of these residues (41/59) are clustered in the activating domain 1 (AD1) of Zap1, which is able to bind multiple Zn^{2+} ions and functions as a zinc-binding sensor domain (Herbig *et al.,* 2005). Similarly, most of the Cys/His residues in ZafA (52/55) are organized into four clusters that could also bind several Zn^{2+} ions (Supporting Information Fig. S4). In addition, ZafA has a tCWCH2 motif that could play a dual role in zinc sensing and DNA binding (Hatayama and Aruga, 2010), similar to the tCWCH2 motif embedded in the AD2 of Zap1 (Bird *et al.,* 2000; Bird *et al.,* 2003). It could also be possible that Zn^{2+} ions binding to the zinc-binding sensor domains causes conformational changes that inactivates the ZafA transcription-activating function, as reported for Zap1 (Bird *et al.,* 2003; Herbig *et al.,* 2005). Moreover, these structural changes could also render ZafA unable to enter the nucleus. It is worth noting that the subcellular location Zap1 does not change in response to zinc availability (Bird *et al.,* 2000), which is consistent with the lack of a NLS similar to that present in ZafA and other transcription factors that typically enter the nucleus upon activation, such as PacC of *Aspergillus* and transcription factors belonging to the metazoan Gli/Glis/Zic superfamily of zinc-finger proteins (Fernández-Martínez *et al.,* 2003; Hatayama and Aruga, 2012). In either case, we posit that the ZafA molecules non-saturated with Zn^{2+} ions under zinc-replete conditions enter the nucleus and bind with a higher probability to the promoter regions of zinc homeostatic genes with the highest number of ZR motifs. It is remarkable that *zrfB*, which is the gene of the *A. fumigatus* genome with the highest number of ZR motifs in its promoter region that is induced by ZafA under zinc-limiting conditions (Vicentefranqueira *et al.,* 2018), is the only zinc homeostatic gene directly targeted by ZafA, whose expression is negatively influenced by HapX under iron-replete conditions. On the other hand, our results are consistent with the notion that HapX directly represses the expression of the SL-mRNA transcripts in zinc-replete media under iron-limiting conditions. Therefore, it is very likely that the HapX-mediated repression of ZafA ultimately results in a reduction of the basal amount of ZafA and, in turn, to a reduction of the *zrfB* expression level. In contrast, the HapX-mediated increase of the expression level of *zrcA* under these circumstances would be an indirect consequence of the non-repression of *zrcA* by ZafA.

One question lies on how HapX can repress the expression of the SL-mRNA transcripts. In the regulatory region of *zafA*, there are two CCAAT-boxes that could recruit HapX through the HapB/C/E proteins of the CCAAT-binding core complex (CBC) in *Aspergillus* (Hortschansky *et al.,* 2017). It has been reported that both the CBC and HapX recognize a conserved bipartite motif in the promoter of *cycA* from *A. nidulans* that has the pseudo-palindromic 3′-submotif 5′-GATGATTCAGC-3′ (Hortschansky *et al.,* 2015). Interestingly, both CCAAT-boxes of the *zafA* promoter have the quasi-palindromic sequence 5′-TGAGTCC/GTG-3′ downstream, which resembles the 3′-submotif that HapX binds to within the *cycA* promoter. Hence, it is likely that HapX down-regulates the expression of the SL-mRNA transcripts under zinc-replete, iron-limiting conditions, through binding to these sequences.

ZafA and HapX contribute to maintaining the steady supply of zinc and iron, respectively, which demands an equilibrated consumption of zinc and iron for optimal fungal growth. We have observed that fungal growth ability is enhanced to a lesser extent by iron in zinc-limiting media than in zinc-replete media (Fig. 2A). Actually, the expression of genes involved in iron uptake is down-regulated in *A. fumigatus* as an adaptive response to growth in zinc-limiting, iron-replete media. This is most likely a mechanism to prevent iron toxicity under zinc

starvation (Vicentefranqueira *et al.,* 2018). In contrast, fungal growth in zinc-replete media (10-100 μM zinc) is strongly conditioned by iron, such that fungal growth decreases when the Zn:Fe ratio of the media becomes >3.2 due to iron shortage (Fig. 2A). However, even under this circumstance, the fungus is able to grow by reducing zinc intake, most likely to prevent the noxious side effects of zinc excess under iron starvation, events that are in concordance with a previous report by other authors (Yasmin *et al.,* 2009). In addition, this is consistent with the fact that the transcription-activating function of both HapX and ZafA is influenced directly by zinc and/or iron depending on the intracellular Zn:Fe ratio. Actually, it is entirely possible that both the ZBDs of ZafA (Supporting Information Fig. S4) and the Cys-rich regions (CRR) of HapX (Gsaller *et al.,* 2014) are able to bind both Zn^{2+} and/or $Fe^{2+/3+}$ ions to different extents depending on the intracellular Zn:Fe ratio. Thus, it would be feasible in zinc-replete media under iron-limiting conditions, when the environmental Zn:Fe ratio is high ($\gg$1.0), that most of the basal amount of ZafA molecules become saturated with Zn^{2+} ions, causing ZafA to become transcriptionally inactive. Similarly, HapX would bind more Zn^{2+} than $Fe^{2+/3+}$ ions, activating its ability to repress the expression of SL-mRNA transcripts (coupled to the up-regulation of the LL-mRNA transcripts), as well as genes encoding iron-requiring proteins or proteins involved in iron detoxification (Gsaller *et al.,* 2014). Conversely, HapX would in parallel induce the expression of genes encoding proteins for iron uptake. Furthermore, it would be feasible in zinc- and iron-replete media, when the Zn:Fe ratio of the media is low (<<1.0), that ZafA binds more $Fe^{2+/3+}$ than Zn^{2+} ions, leading to the activation of the basal amount of ZafA molecules. Similarly, most molecules of the basal amount of HapX synthesized in iron-replete media (Gsaller *et al.,* 2014) would bind more $Fe^{2+/3+}$ than Zn^{2+} ions, enabling it to enhance SL-mRNA expression. At the same time, genes encoding proteins involved in iron detoxification would also be enhanced, while the ability of HapX to induce genes encoding iron-requiring proteins or those involved in iron uptake would be reduced. Importantly, this hypothetical opposite regulatory effect of HapX on the expression of the SL-mRNA transcripts would not be unexpected given the functional duality attributed to HapX as an activator/repressor in *A. fumigatus* depending on iron availability (Gsaller *et al.,* 2014).

Finally, to explain how ZafA mediates the reduction of zinc intake from zinc-replete media under iron-limiting conditions, we propose a model that relies on the HapX-mediated regulation of the L-transcription subunits of *zafA* under zinc-replete conditions. We propose that the selection of the TSS of the L-transcripts is influenced directly by HapX. Under iron-limiting conditions, HapX repress the expression of the SL-transcripts leading automatically to the transcription of the LL-transcripts. Moreover, the high number of out-of-frame AUG codons in the 5'-UTRs of the LL-transcripts may provide the structural basis to reduce their translational efficiency through a leaky scanning mechanism (Wang and Rothnagel, 2004; Araujo *et al.,* 2012). As a result, under iron-limiting conditions, an exceedingly low basal amount of ZafA is synthesized leading to a reduction in zinc intake and, hence, to prevent the noxious side effects caused by an intracellular excess of zinc during iron starvation. In contrast, the low amount of HapX under iron-replete conditions would favour the expression of the SL-mRNA transcripts, whose translation produces a basal amount of ZafA higher than that produced under iron-limiting conditions, increasing the intake of zinc and enhancing fungal growth. Moreover, the activated basal amount of ZafA might also contribute to the repression of LL-mRNA expression, since the major TSS sites for the LL-mRNA transcripts are located within (and upstream) the ZRR3 motif to which ZafA is able to bind with high affinity (Fig. 4B) (Vicentefranqueira *et al.,* 2018).

In summary, we have shown that iron availability determines the basal amount of ZafA that is synthesized under zinc-replete conditions by an unprecedented mechanism that involves the iron-dependent expression of different transcription subunits of *zafA.* This regulatory mechanism may have evolved to enhance the ability of the fungus to grow when the Zn:Fe ratio of the medium is adequate and to restrict it by reducing zinc intake when iron becomes scarce to prevent the noxious side effects of a relatively high intracellular amount of zinc under iron deficiency.

Experimental procedures

Strains and culture conditions

The *A. fumigatus* strains used in this study are listed in Table 1. Fresh conidia used as inoculum were harvested from fungal strains grown in PDA (Moreno *et al.*, 2007a). All liquid culture media were inoculated to a density of 1.5×10^6 spores/mL and incubated at 37°C with shaking at 200 rpm for 20 h. Most cultures were carried out in the Synthetic Dextrose Nitrate Zinc- and Iron-limiting medium (SDN–Zn–Fe, pH ~7.5) (1.7 g/l YNB without amino acids, without ammonium sulphate and without zinc [CYN2401, Formedium], 20 g/l Dextrose, 3 g/l $NaNO_3$, 2 μM $CuSO_4$-5 H_2O, 2 μM Na_2MoO_4-2 H_2O). The SDN–Zn–Fe medium contains 0.74 μM iron (as $FeCl_3$). The SDN–Zn–Fe was supplemented with zinc ($ZnSO_4$-7H_2O) and/or iron ($FeSO_4$–7 H_2O) as specified.

The AMM for microscopy (A3M) contained 10 g/l Dextrose, 0.3 g/l $NaNO_3$, 0.052 g/l $MgSO_4$–7H_2O, 0.052 g/l KCl, 0.152 g/l KH_2PO_4 and 0.1 ml/l Cove's trace-element solution without $ZnSO_4$ and with 1.2 g/l $FeSO_4$-7 H_2O

Table 1. *Aspergillus fumigatus* strains used in this study.

Strain	Genotype	Reference
CEA10	Wild type	(d'Enfert, 1996)
CEA17	*pyrG1* (auxotrophic PyrG$^-$)	(d'Enfert, 1996)
AF14	Wild-type[a]	(Vicentefranqueira *et al.,* 2005)
HH1	Δ*hapX::hph*	(Blatzer *et al.,* 2011)
HH6	Δ*sreA::hph*	(Blatzer *et al.,* 2011)
RC1	Δ*srbA::pyrG*	(Willger *et al.,* 2008)
RC2	Δ*srbB::pyrG*	(Chung *et al.,* 2014)
AF171	Δ*zafA::hisG*[a]	(Moreno *et al*., 2007b)
AF1031	Δ*zafA::GFP-PpyrG-pyrG-PpyrG*	This study
AF1041	Δ*zafA::GFP-PpyrG* (auxotrophic PyrG$^-$)	This study
AF1043	Δ*zafA::GFP-PpyrG* [P*zafA*^{wt} → *myc-zafA*][a,b]	This study
AF1045	Δ*zafA::GFP-PpyrG* [P*actA* → *myc-zafA*][a,b]	This study
AF1047	Δ*zafA::GFP GFP-zafA-pyrG-PpyrG*	This study
AF1059	Wild type [P*actA* → *zrfC*]	This study

a. Isogenic to CEA17.
b. Genes in brackets were reintroduced into the *A. fumigatus* genome by targeting them at the intergenic region between the AFUA_2G08360 (*pyrG*) and AFUA_2G08350 genes.

instead of 0.8 g/l $FePO_4$-2 H_2O (Cove, 1966). The pH was adjusted to 6.5 with NaOH.

Molecular biology techniques

Oligonucleotides used to obtain DNA probes by PCR, for reverse transcription and qPCR experiments are listed in Supporting Information Table S1. The purification and analysis of RNA by Northern blot and RT-qPCR was performed as previously described (Vicentefranqueira *et al.,* 2005; Vicentefranqueira *et al.,* 2018). Genomic DNA from *A. fumigatus* was obtained and analysed by Southern blot as previously described (Amich *et al.,* 2009).

The identification of the 3′-ends of the *zafA* mRNAs was performed by 3'-RACE. The DNase-treated RNA was reversed transcribed at 52°C for 45 min using the SuperScript III Reverse Transcriptase (Invitrogen, cat. No. 18064-093) and the oligo $(dT)_{15}$ primer (C1101, Promega). Next, PCR was performed using the oligonucleotide pair JA429/A3CE-T followed by a nested PCR using the primer pair JA487/A3CE. The nested PCR products were cloned into pGEM-T-easy. Several tens of independent colonies of *Escherichia coli* were analysed by PCR using universal forward and reverse primers (Fw/Rev). All plasmids carrying a PCR fragment larger than ~700 bp, which was the minimal expected size of the cDNA fragment amplified by PCR, were isolated and sequenced. The results obtained have been summarized in a table (Supporting Information Fig. S1A).

To identify the 5′-ends of the different populations of mRNAs of *zafA*, we used a procedure based on recircularization of reversed transcribed 5′-phosphorylated cDNAs (Dallmeier and Neyts, 2013). The DNase-treated RNA was reversed transcribed at 52°C for 45 min using the SuperScript III Reverse Transcriptase and a 5′-phosphorylated oligonucleotide as the primer. The reaction was inactivated at 95°C for 15 min, and RNA was removed using a mix of RNase A plus RNase T at 37°C for 30 min. The cDNA was precipitated with 0.1 vol 3.0 M NaAc (pH 5.2) and 2.5 volumes of 100% ethanol at −20°C for 12 h and washed with 70% (v/v) ethanol. The cDNA was air dried, resuspended in 11.5 μl of water and recircularized using CircLigase by adding to 2 μl 10× CircLigase buffer, 1 μl of 50 mM $MnCl_2$, 4 μl of 5 mM betaine and 1.5 μl of CircLigase II ssDNA (100 U/μl). The reaction was incubated at 60°C for 12 h, and the enzyme was inactivated at 80°C for 10 min. The recircularized cDNA fragments were digested with 1 μl of exonuclease I (20 U/μL) and 0.5 μl of exonuclease III (200 U/μL) at 37°C for 50 min and the exonucleases were inactivated at 85°C for 15 min. These reactions were used for standard PCR. Each PCR reaction included 5 μl of the recircularization reaction and a pair of divergent oligonucleotides. Three different sets of oligonucleotides were used: Set A (oligonucleotides JA428*, JA429 and JA430), set B (JA425*, JA438 and JA439) and set C (JA431*, JA124 and JA432) (the oligonucleotides labelled with an asterisk were phosphorylated at their 5′-end). The PCR fragments were cloned into pGEM-T-easy. Several hundreds of independent colonies of *E. coli* were analysed by PCR using Fw/Rev primers. All plasmids carrying a PCR fragment larger than ~245 bp, which was the minimal expected size of the DNA fragment amplified by PCR, were isolated and sequenced. The results obtained for the 5'-TSSs of the S- and L-mRNAs have been compiled in their corresponding tables (Supporting Information Fig. S1B).

Construction of the A. fumigatus mutants and the transforming DNA fragments used to generate them

DNA fragments obtained from plasmids pZAF472, pZAF474, pZAF96, pZAF97 and pZRF396 were used to generate, respectively, the strains AF1031, AF1047, AF1043, AF1045 and AF1059 after transforming protoplasts of the appropriated PyrG$^-$ uracil-uridine-auxotrophic strains of *A. fumigatus*, as described previously (Vicentefranqueira *et al.,* 2018).

A DNA fragment carrying the *PpyrG-pyrG-PpyrG* selection marker cassette, preceded by the coding sequence of sGFP (Fernández-Ábalos *et al.,* 1998), was used to generate pZAF472 by replacing the *zafA* coding sequence in pZAF48 (Moreno *et al.*, 2007b). The plasmid pZAF474 was constructed by introducing the coding

sequence of *zafA* in frame with that of the sGFP into pZAF472. Hence, pZAF474 carried the *GFP-zafA* coding sequence preceded by the [AFUA_1G10060 — AFUA_1G10080/*zafA*] intergenic sequence that harboured both the 5′-UTRs of the *zafA* transcripts and the *zafA* promoter region.

The pZAF96 and pZAF97 plasmids carried a *myc*-tagged version of the *zafA* coding sequence whose expression was driven by the wild-type *zafA* promoter [P*zafA* → *myc-zafA*] and the promoter of the *actA* gene from *A. nidulans* [P*actA* → *myc-zafA*] (Fidel *et al.,* 1988), respectively. The pZRF396 plasmid carried the *zrfC* coding sequence under the control of the *actA* promoter from *A. nidulans* [P*actA* → *zrfC*]. These plasmids allowed us to introduce DNA fragments at the *pyrG* locus of any uracil-uridine-auxotrophic PyrG$^-$ strain.

Western blot protein analysis

Mycelia were harvested by filtration, washed with sterile water and snap-frozen in liquid nitrogen. Approximately 100 mg of mycelium (wet weight) was grounded using a mortar and pestle in liquid N_2 until it became a fine powder and was used to prepare protein extracts as previously described (Lucena-Agell *et al.,* 2015).

For Western blot analyses, the proteins were transferred to a PVDF membrane at 300 mA for 1 h. An anti-*c-myc*-peroxidase mouse monoclonal antibody (clone 9E10) conjugated to peroxidase (Roche, Cat. No. 11814150001) (dilution 1:5000) was used to detect the Myc3×-tagged ZafA protein, and GFP was detected using the anti-GFP mouse monoclonal antibody (BD living colours JL-8, ref. 8371-2) (1:10,000) as the primary antibody and the anti-mouse IgG (H + L)-Peroxidase antibody (Enzo life sciences, ref. VC-PI-2000-M001) (1:10,000) as the secondary antibody. Actin was detected using the anti-actin (20-30) IgG fraction of antiserum that recognizes an N-terminal epitope (residues 20-34) of actin (Sigma, A5060) (1:1000) as the primary antibody and the anti-rabbit IgG (H + L)-Peroxidase antibody (BioRad ref. 170-6515) (1:10,000) as the secondary antibody. The blots were developed using the WesternBright ECL chemiluminescent substrate kit (Advansta, K-12045-D50).

*qPCR-based procedure to quantify the different transcripts of (*myc*)*zafA*, GFP and* zrfC

The REL of each type of mRNA from *zafA* in a wild-type strain (AF14 or CEA10) was estimated by RT-qPCR using three pairs of oligonucleotides for each cDNA sample and the 18S rRNA as an internal reference (Supporting Information Fig. S9, upper panel). These pairs of oligonucleotides (LL-Fw1/LL-Rv1, SL-Fw/SL-Rv and ZAFA-D5/ZAFA-R5) were carefully designed for obtaining efficiency values between 98.9% and 99.8%, as calculated by qPCR using 1:10 serial dilutions of gDNA (ranging from 10^0 to 10^{-5}). The pair of oligonucleotides LL-Fw1/LL-Rv1 was used to detect exclusively the LL-transcripts, because it amplifies a cDNA fragment that is only present in the LL-mRNA and the corresponding $2^{-\Delta Ct}$ value was designated as '*a*'. The pair of oligonucleotides SL-Fw/SL-Rv was used to amplify a cDNA fragment present in all LL-mRNA and SL-mRNA transcripts and the corresponding $2^{-\Delta Ct}$ value was designated as '*b*'. The pair of oligonucleotides ZAFA-D5/ZAFA-R5 was used to amplify a cDNA fragment present in all *zafA* transcripts (LL-, SL- and S-mRNA) (Supporting Information Fig. S9, upper panel) and the corresponding $2^{-\Delta Ct}$ value was designated as '*c*'. We estimated in a wild-type strain that the relative amount of LL-mRNA = a, SL-mRNA = $(b - a)$ and S-mRNA = $(c - b)$. To determine the percentage of each type of *zafA* transcript in a wild-type strain, we considered that the total amount of *zafA* transcripts in a sample was defined by the $2^{-\Delta Ct}$ value calculated using the pair of oligonucleotides ZAFA-D5/ZAFA-R5, which was designated as '*c*', such that %LL-mRNA = $100 \times a/c$, %SL-mRNA = $100 \times (b - a)/c$ and %S-mRNA = $100 \times (c - b)/c$.

The REL of each type of mRNA for *zafA* and GFP in the AF1043 strain was estimated by RT-qPCR using four different pairs of oligonucleotides for each cDNA sample and the 18S rRNA as an internal reference (REL/18S). The pairs of oligonucleotides LL-Fw1/LL-Rv1 was used to detect both the LL-mRNA$^{myc\text{-}zafA}$ and LL-mRNA^{gfp} transcripts and the corresponding $2^{-\Delta Ct}$ value was designated as '*a*'. The pair of oligonucleotides SL-Fw/SL-Rv was used to detect all LL and SL-cDNAs (i.e., LL$^{myc\text{-}zafA}$, LL^{gfp}, SL$^{myc\text{-}zafA}$ and SL^{gfp}) and the corresponding $2^{-\Delta Ct}$ value was designated as '*b*'. The pair of oligonucleotides ZAFA-D5/ZAFA-R5 was used to amplify specifically all *myc-zafA* transcripts and the corresponding $2^{-\Delta Ct}$ value was designated as '*c*' (Supporting Information Fig. S9, upper panel). The pair of oligonucleotides qGFP2-D/qGFP2-R was used specifically to amplify a cDNA fragment present in all GFP mRNAs and the corresponding $2^{-\Delta Ct}$ value was designated as '*d*' (Supporting Information Fig. S9, lower panel). The total amount of S-transcripts in a cDNA sample from the AF1043 strain for both *zafA* and GFP was $(c + d)$, whereas the mRNA$^{myc\text{-}zafA}$ ratio = $c/(c + d)$ and the mRNA^{gfp} ratio = $d/(c + d)$. Hence, we estimated that, in the AF1043 strain, the amount of LL-mRNA$^{myc\text{-}zafA}$ = $a \times c/(c + d)$, LL-mRNA^{gfp} = $a \times d/(c + d)$, SL-mRNA$^{myc\text{-}zafA}$ = $(b - a) \times c/(c + d)$, SL-mRNA^{gfp} = $(b - a) \times d/(c + d)$, S-mRNA$^{myc\text{-}zafA}$ = $c - [c \times b/(c + d)]$ and S-mRNA^{gfp} = $d - [d \times b/(c + d)]$. To determine the percentage of each type of *zafA*/GFP transcript in the AF1043 strain, it was considered that the total

amount of (*zafA* + GFP) transcripts in a sample was defined by the sum of the $2^{-\Delta Ct}$ values calculated using the pairs of oligonucleotides ZAFA-D5/ZAFA-R5 and qGFP2-D/qGFP2-R that were designated, respectively, as '*c*' and '*d*', such that %LL-mRNA$^{myc\text{-}zafA}$ = 100 × [$a \times c/(c + d)^2$], %LL-mRNA^{gfp} = 100 × [$a \times d/(c + d)^2$], %SL-mRNA$^{myc\text{-}zafA}$ = 100 × [$(b - a) \times c/(c + d)^2$], %SL-mRNA^{gfp} = 100 × [$(b - a) \times d/(c + d)^2$], %S-mRNA$^{myc\text{-}zafA}$ = 100 × [$c \times (c + d - b)/(c + d)^2$] and %S-mRNA^{gfp} = 100 × [$d \times (c + d - b)/(c + d)^2$].

The REL of each type of mRNA for GFP in the AF1031 strain was estimated by RT-qPCR using three pairs of oligonucleotides (LL-Fw1/LL-Rv1, SL-Fw/SL-Rv and qGFP2-D/qGFP2-R) for each cDNA sample and the 18S rRNA as an internal reference (Supporting Information Fig. S9, lower panel). The $2^{-\Delta Ct}$ values calculated using the pair of oligonucleotides LL-Fw1/LL-Rv1, SL-Fw/SL-Rv and qGFP2-D/qGFP2-R were designated, respectively, as '*a*', '*b*' and '*d*'. Thus, we estimated that, in the AF1031 strain, the amount of LL-mRNA^{gfp} = *a*, SL-mRNA^{gfp} = $(b - a)$ and S-mRNA^{gfp} = $(d - b)$. To determine the percentage of each type of GFP transcript in the AF1031 strain, it was considered that the total amount of GFP transcripts in a sample was defined by the $2^{-\Delta Ct}$ value calculated using the pair of oligonucleotides qGFP2-D/qGFP2-R that was designated as '*d*', such that %LL-mRNA^{gfp} = 100 × a/d, %SL-mRNA^{gfp} = 100 × $(b - a)/d$ and %S-mRNA^{gfp} = 100 × $(d - b)/d$.

The REL of the *zrfC* mRNA transcribed in the original *zrfC* locus of the AF1059 strain (*zrfC*^{wt}) was estimated by RT-qPCR using the pair of oligonucleotides ZRFC-D1/ZRFC-R1, whereas the REL of the *zrfC* mRNA transcribed constitutively in the *pyrG* locus (under the control of the *actA* promoter from *A. nidulans*) of the AF1059 strain (*zrfC*^{c}) was estimated by RT-qPCR using the pair of oligonucleotides ZRFC-D1/PYRG-R1 (Supporting Information Fig. S8A). The REL of the total *zrfC* mRNA transcripts expressed in the AF1059 strain (i.e., *zrfC*^{wt} + *zrfC*^{c}) was estimated by RT-qPCR using the pair of oligonucleotides ZRFC-D2/ZRFC-R2. In all cases, the 18S rRNA was used as an internal reference. The $2^{-\Delta Ct}$ values calculated using the pair of oligonucleotides ZRFC-D1/ZRFC-R1, ZRFC-D1/PYRG-R1 and ZRFC-D2/ZRFC-R2 were designated, respectively, as '*a*', '*b*' and '*c*' such that in the AF1059 strain, the amount of *zrfC*^{wt} = *a*, *zrfC*^{c} = *b* and *zrfC*^{wt} + *zrfC*^{c} = *c*.

Acknowledgements

This work was supported by the Ministry of Economy and Competitiveness (Spain) and The Education Council of the Regional Government of Castile & Leon (Spain) through grants SAF2013-48382-R and SA020G18 respectively awarded to JAC. We are grateful to Hubertus Haas and Robert Cramer for kindly providing fungal mutant strains. RV was supported by a contract made possible through grant SAF2013-48382-R; CIS was supported by a fellowship from the Industrial University of Santander (Bucaramanga, Colombia) through resolution n° 2604 (December, 2014).

References

Amich, J., and Calera, J.A. (2014) Zinc acquisition: a key aspect in *Aspergillus fumigatus* virulence. *Mycopathologia* **178**: 379–385.

Amich, J., Leal, F., and Calera, J.A. (2009) Repression of the acid ZrfA/ZrfB zinc-uptake system of *Aspergillus fumigatus* mediated by PacC under neutral, zinc-limiting conditions. *Int Microbiol* **12**: 39–47.

Amich, J., Vicentefranqueira, R., Leal, F., and Calera, J.A. (2010) *Aspergillus fumigatus* survival in alkaline and extreme zinc-limiting environments relies on the induction of a zinc homeostasis system encoded by the *zrfC* and *aspf2* genes. *Eukaryot Cell* **9**: 424–437.

Amich, J., Vicentefranqueira, R., Mellado, E., Ruiz-Carmuega, A., Leal, F., and Calera, J.A. (2014) The ZrfC alkaline zinc transporter is required for *Aspergillus fumigatus* virulence and its growth in the presence of the Zn/Mn-chelating protein calprotectin. *Cell Microbiol* **16**: 548–564.

Andreini, C., Bertini, I., Cavallaro, G., Holliday, G.L., and Thornton, J.M. (2008) Metal ions in biological catalysis: from enzyme databases to general principles. *J Biol Inorg Chem* **13**: 1205–1218.

Araujo, P.R., Yoon, K., Ko, D., Smith, A.D., Qiao, M., Suresh, U., *et al.* (2012) Before it gets started: regulating translation at the 5' UTR. *Comp Funct Genomics* **2012**: 475731.

Auld, D.S. (2009) The ins and outs of biological zinc sites. *Biometals* **22**: 141–148.

Bird, A.J., McCall, K., Kramer, M., Blankman, E., Winge, D. R., and Eide, D.J. (2003) Zinc fingers can act as Zn^{2+} sensors to regulate transcriptional activation domain function. *EMBO J* **22**: 5137–5146.

Bird, A.J., Zhao, H., Luo, H., Jensen, L.T., Srinivasan, C., Evans-Galea, M., *et al.* (2000) A dual role for zinc fingers in both DNA binding and zinc sensing by the Zap1 transcriptional activator. *EMBO J* **19**: 3704–3713.

Blatzer, M., Barker, B.M., Willger, S.D., Beckmann, N., Blosser, S.J., Cornish, E.J., *et al.* (2011) SREBP coordinates iron and ergosterol homeostasis to mediate triazole drug and hypoxia responses in the human fungal pathogen *Aspergillus fumigatus*. *PLoS Genet* **7**: e1002374.

Chung, D., Barker, B.M., Carey, C.C., Merriman, B., Werner, E.R., Lechner, B.E., *et al.* (2014) ChIP-seq and *in vivo* transcriptome analyses of the *Aspergillus fumigatus* SREBP SrbA reveals a new regulator of the fungal hypoxia response and virulence. *PLoS Pathog* **10**: e1004487.

Cove, D.J. (1966) The induction and repression of nitrate reductase in the fungus *Aspergillus nidulans*. *Biochim Biophys Acta* **113**: 51–56.

d'Enfert, C. (1996) Selection of multiple disruption events in *Aspergillus fumigatus* using the orotidine-5′-decarboxylase

gene, *pyrG*, as a unique transformation marker. *Curr Genet* **30**: 76–82.

Dallmeier, K., and Neyts, J. (2013) Simple and inexpensive three-step rapid amplification of cDNA 5′ ends using 5′ phosphorylated primers. *Anal Biochem* **434**: 1–3.

Eide, D.J. (2009) Homeostatic and adaptive responses to zinc deficiency in *Saccharomyces cerevisiae*. *J Biol Chem* **284**: 18565–18569.

Fernández-Ábalos, J.M., Fox, H., Pitt, C., Wells, B., and Doonan, J.H. (1998) Plant-adapted green fluorescent protein is a versatile vital reporter for gene expression, protein localization and mitosis in the filamentous fungus, *Aspergillus nidulans*. *Mol Microbiol* **27**: 121–130.

Fernández-Martínez, J., Brown, C.V., Diez, E., Tilburn, J., Arst, H.N., Jr., Peñalva, M.A., and Espeso, E.A. (2003) Overlap of nuclear localisation signal and specific DNA-binding residues within the zinc finger domain of PacC. *J Mol Biol* **334**: 667–684.

Fidel, S., Doonan, J.H., and Morris, N.R. (1988) *Aspergillus nidulans* contains a single actin gene which has unique intron locations and encodes a gamma-actin. *Gene* **70**: 283–293.

Gsaller, F., Hortschansky, P., Beattie, S.R., Klammer, V., Tuppatsch, K., Lechner, B.E., *et al.* (2014) The Janus transcription factor HapX controls fungal adaptation to both iron starvation and iron excess. *EMBO J* **33**: 2261–2276.

Hatayama, M., and Aruga, J. (2010) Characterization of the tandem CWCH2 sequence motif: a hallmark of inter-zinc finger interactions. *BMC Evol Biol* **10**: 53.

Hatayama, M., and Aruga, J. (2012) Gli protein nuclear localization signal. *Vitam Horm* **88**: 73–89.

Herbig, A., Bird, A.J., Swierczek, S., McCall, K., Mooney, M., Wu, C.Y., *et al.* (2005) Zap1 activation domain 1 and its role in controlling gene expression in response to cellular zinc status. *Mol Microbiol* **57**: 834–846.

Hortschansky, P., Ando, E., Tuppatsch, K., Arikawa, H., Kobayashi, T., Kato, M., *et al.* (2015) Deciphering the combinatorial DNA-binding code of the CCAAT-binding complex and the iron-regulatory basic region leucine zipper (bZIP) transcription factor HapX. *J Biol Chem* **290**: 6058–6070.

Hortschansky, P., Haas, H., Huber, E.M., Groll, M., and Brakhage, A.A. (2017) The CCAAT-binding complex (CBC) in *Aspergillus* species. *Biochim Biophys Acta* **1860**: 560–570.

Karthaus, M., and Buchheidt, D. (2013) Invasive aspergillosis: new insights into disease, diagnostic and treatment. *Curr Pharm Des* **19**: 3569–3594.

Lucena-Agell, D., Galindo, A., Arst, H.N., Jr., and Peñalva, M.A. (2015) *Aspergillus nidulans* ambient pH signaling does not require endocytosis. *Eukaryot Cell* **14**: 545–553.

Mateus, C., and Avery, S.V. (2000) Destabilized green fluorescent protein for monitoring dynamic changes in yeast gene expression with flow cytometry. *Yeast* **16**: 1313–1323.

Moreno, M.A., Amich, J., Vicentefranqueira, R., Leal, F., and Calera, J.A. (2007a) Culture conditions for zinc- and pH-regulated gene expression studies in *Aspergillus fumigatus*. *Int Microbiol* **10**: 187–192.

Moreno, M.A., Ibrahim-Granet, O., Vicentefranqueira, R., Amich, J., Ave, P., Leal, F., *et al.* (2007b) The regulation of zinc homeostasis by the ZafA transcriptional activator is essential for *Aspergillus fumigatus* virulence. *Mol Microbiol* **64**: 1182–1197.

Outten, C.E., and O'Halloran, T.V. (2001) Femtomolar sensitivity of metalloregulatory proteins controlling zinc homeostasis. *Science* **292**: 2488–2492.

Schrettl, M., Beckmann, N., Varga, J., Heinekamp, T., Jacobsen, I.D., Jochl, C., *et al.* (2010) HapX-mediated adaption to iron starvation is crucial for virulence of *Aspergillus fumigatus*. *PLoS Pathog* **6**: e1001124.

Schrettl, M., Kim, H.S., Eisendle, M., Kragl, C., Nierman, W. C., Heinekamp, T., *et al.* (2008) SreA-mediated iron regulation in *Aspergillus fumigatus*. *Mol Microbiol* **70**: 27–43.

Vicentefranqueira, R., Amich, J., Marín, L., Sánchez, C.I., Leal, F., and Calera, J.A. (2018) The transcription factor ZafA regulates the homeostatic and adaptive response to zinc starvation in *Aspergillus fumigatus*. *Genes* **9**: 318.

Vicentefranqueira, R., Moreno, M.A., Leal, F., and Calera, J. A. (2005) The *zrfA* and *zrfB* genes of *Aspergillus fumigatus* encode the zinc transporter proteins of a zinc uptake system induced in an acid, zinc-depleted environment. *Eukaryot Cell* **4**: 837–848.

Wang, X.Q., and Rothnagel, J.A. (2004) 5′-untranslated regions with multiple upstream AUG codons can support low-level translation via leaky scanning and reinitiation. *Nucleic Acids Res* **32**: 1382–1391.

Willger, S.D., Puttikamonkul, S., Kim, K.H., Burritt, J.B., Grahl, N., Metzler, L.J., *et al.* (2008) A sterol-regulatory element binding protein is required for cell polarity, hypoxia adaptation, azole drug resistance, and virulence in Aspergillus fumigatus. *PLoS Pathog* **4**: e1000200.

Wingender, E. (2013) Criteria for an updated classification of human transcription factor DNA-binding domains. *J Bioinform Comput Biol* **11**: 1340007.

Xu, D., Marquis, K., Pei, J., Fu, S.C., Cagatay, T., Grishin, N.V., and Chook, Y.M. (2015) LocNES: a computational tool for locating classical NESs in CRM1 cargo proteins. *Bioinformatics* **31**: 1357–1365.

Yasmin, S., Abt, B., Schrettl, M., Moussa, T.A., Werner, E. R., and Haas, H. (2009) The interplay between iron and zinc metabolism in *Aspergillus fumigatus*. *Fungal Genet Biol* **46**: 707–713.

Zhao, H., and Eide, D.J. (1997) Zap1p, a metalloregulatory protein involved in zinc-responsive transcriptional regulation in *Saccharomyces cerevisiae*. *Mol Cell Biol* **17**: 5044–5052.

Supporting Information

Additional Supporting Information may be found in the online version of this article at the publisher's web-site:

Appendix S1: Supplementary Information